



Measurement of azimuthal anisotropy of muons from charm and bottom hadrons in Pb+Pb collisions at $\sqrt{s_{NN}} = 5.02$ TeV with the ATLAS detector

The ATLAS Collaboration*

ARTICLE INFO

Article history:

Received 8 March 2020

Received in revised form 10 June 2020

Accepted 24 June 2020

Available online 29 June 2020

Editor: M. Doser

ABSTRACT

Azimuthal anisotropies of muons from charm and bottom hadron decays are measured in Pb+Pb collisions at $\sqrt{s_{NN}} = 5.02$ TeV. The data were collected with the ATLAS detector at the Large Hadron Collider in 2015 and 2018 with integrated luminosities of 0.5 nb^{-1} and 1.4 nb^{-1} , respectively. The kinematic selection for heavy-flavor muons requires transverse momentum $4 < p_T < 30$ GeV and pseudorapidity $|\eta| < 2.0$. The dominant sources of muons in this p_T range are semi-leptonic decays of charm and bottom hadrons. These heavy-flavor muons are separated from light-hadron decay muons and punch-through hadrons using the momentum imbalance between the measurements in the tracking detector and in the muon spectrometers. Azimuthal anisotropies, quantified by flow coefficients, are measured via the event-plane method for inclusive heavy-flavor muons as a function of the muon p_T and in intervals of Pb+Pb collision centrality. Heavy-flavor muons are separated into contributions from charm and bottom hadron decays using the muon transverse impact parameter with respect to the event primary vertex. Non-zero elliptic (v_2) and triangular (v_3) flow coefficients are extracted for charm and bottom muons, with the charm muon coefficients larger than those for bottom muons for all Pb+Pb collision centralities. The results indicate substantial modification to the charm and bottom quark angular distributions through interactions in the quark-gluon plasma produced in these Pb+Pb collisions, with smaller modifications for the bottom quarks as expected theoretically due to their larger mass.

© 2020 The Author(s). Published by Elsevier B.V. This is an open access article under the CC BY license (<http://creativecommons.org/licenses/by/4.0/>). Funded by SCOAP³.

1. Introduction

The paradigm for the time evolution of heavy-ion collisions at the Relativistic Heavy Ion Collider (RHIC) and the Large Hadron Collider (LHC) involves the formation and hydrodynamic expansion of a region of hot and dense quark–gluon plasma (QGP) with a small ratio of the shear viscosity to entropy density. In this paradigm, the QGP is considered to be a nearly perfect fluid [1,2]. Initial geometric inhomogeneities of the QGP are translated into momentum anisotropies of the final-state hadrons via large pressure gradients. Extensive measurements of light-hadron azimuthal anisotropies have been performed, in which the single-particle azimuthal distributions are expressed in terms of a Fourier expansion:

$$\frac{dN}{d\phi} \propto 1 + 2 \sum_{n=1}^{\infty} v_n \cos(n(\phi - \Psi_n)), \quad (1)$$

where the event-plane angle, Ψ_n , specifies the orientation of the initial density profile in the transverse plane [3], and Fourier coefficients, v_n , quantify the magnitude of the modulation with respect to the event-plane angle. The second- and third-order v_n coefficients are referred to as elliptic (v_2) and triangular (v_3) flow coefficients, respectively, with the term ‘flow’ invoking the hydrodynamic paradigm.

Heavy-flavour (charm and bottom) quarks have masses much larger than the temperature of the QGP ($m_{c,b} > T$), with maximum temperatures at early times ranging between 300 and 500 MeV [4]. Thus, thermal production of heavy quarks during the QGP phase is highly suppressed. Instead, heavy quarks are typically produced at the earliest times via high-momentum-transfer collisions between incoming partons. Once created, the heavy quarks persist throughout the dynamical time evolution of the QGP and thus act as sensitive probes of the hot and dense medium.

Owing to their larger masses, radiative energy loss of heavy quarks in the QGP is suppressed relative to that of light quarks [5]. However, it was still postulated that charm quarks interact strongly enough to flow with the QGP [6]. Experimental data at RHIC and then at the LHC reveals that heavy-quark hadrons, as well as their decay leptons, have transverse momentum (p_T) distributions

* E-mail address: atlas.publications@cern.ch.

that are strongly modified by the QGP relative to observations in proton–proton (pp) collisions [7–12]. Charm hadrons [13,14] and heavy-quark hadron decay leptons [7,15] are also observed to have significant azimuthal anisotropies, suggesting that they participate in the overall collective flow of the medium. For recent reviews of heavy-flavour measurements in heavy-ion collisions, see Refs. [16–18].

For $p_T \lesssim 4\text{--}6$ GeV, it was proposed that heavy quarks can be described via a Langevin approach with drag and diffusion terms [19]. Modified p_T distributions and azimuthal anisotropies of D mesons have been used to constrain heavy-quark transport coefficients [20,21]. Other models of heavy-flavor kinematics in the QGP, including a Boltzmann approach, have also been explored [22–26]. At higher momenta $p_T \gtrsim 5\text{--}10$ GeV, heavy-quark energy loss is thought to dominate, with collisional and induced radiative processes both contributing [27]. At intermediate p_T hadronization effects can be important as azimuthal anisotropies for the deconfined heavy-quark is transferred to the heavy-flavor hadron [28]. There are numerous theoretical predictions for the azimuthal anisotropies of bottom quarks, e.g. in Refs. [29–31]; however, only limited experimental data are currently available. Precision experimental data for p_T distributions and azimuthal anisotropies is crucial as this over-constrains the calculations that depend on the heavy-quark to QGP coupling as well as the QGP space-time evolution.

The flow coefficients v_2 , v_3 , and v_4 of inclusive heavy-flavour muon production, which includes both muons from charm hadron decays (“charm muons”) and muons from bottom hadron decays (“bottom muons”), have been measured by the ATLAS experiment [7] and ALICE experiment [32] in Pb+Pb collisions at $\sqrt{s_{NN}} = 2.76$ TeV. The measurement indicates significant elliptic flow for heavy-flavour muons with $4 < p_T < 10$ GeV. Recently, the heavy-flavour muon v_2 has also been measured in high-multiplicity $\sqrt{s} = 13$ TeV pp collisions [33]. Unlike the earlier Pb+Pb measurement, the pp measurement examined charm muons and bottom muons separately, finding a non-zero v_2 for charm muons while the v_2 for bottom muons is consistent with zero within uncertainties.

In the measurement presented in this paper, the procedure of the previous $\sqrt{s_{NN}} = 2.76$ TeV Pb+Pb analysis using the event-plane method is followed [7], and is extended to extract separate flow coefficients for charm and bottom muons. These measurements extends the previously published ones to the higher $\sqrt{s_{NN}} = 5.02$ TeV Pb+Pb beam energy, using a larger event sample provided by the 2015 and 2018 combined data sets. The larger data sample enables measurements over a larger momentum range $4 < p_T < 30$ GeV for inclusive heavy-flavour muons. It also allows the separation of the inclusive heavy-flavour muons into charm and bottom contributions. Results for charm and bottom muon elliptic v_2 and triangular v_3 flow coefficients are presented as a function of muon p_T for various ranges of overlap between the colliding nuclei, referred to as “centrality”.

2. ATLAS detector

The ATLAS detector [34–36] at the LHC is a multipurpose particle detector with a forward–backward symmetric cylindrical geometry and a near 4π coverage in solid angle.¹ It consists of an inner tracking detector surrounded by a thin superconducting solenoid

providing a 2 T axial magnetic field, electromagnetic and hadron calorimeters, and a muon spectrometer. The inner tracking detector (ID) covers the pseudorapidity range $|\eta| < 2.5$. It consists of silicon pixel, silicon microstrip, and transition radiation tracking (TRT) detectors. The calorimeter system covers the pseudorapidity range $|\eta| < 4.9$. Within the region $|\eta| < 3.2$, electromagnetic calorimetry is provided by barrel and endcap high-granularity lead/liquid-argon (LAr) calorimeters, with an additional thin LAr presampler covering $|\eta| < 1.8$, to correct for energy loss in material upstream of the calorimeters. Hadronic calorimetry is provided by the steel/scintillator-tile calorimeter, segmented into three barrel structures within $|\eta| < 1.7$, and two copper/LAr hadronic endcap calorimeters. The solid angle coverage is completed with forward copper/LAr and tungsten/LAr calorimeter modules (FCal) optimised for electromagnetic and hadronic measurements respectively. The muon spectrometer (MS) comprises separate trigger and high-precision tracking chambers, covering $|\eta| < 2.4$ and $|\eta| < 2.7$ respectively, and measures the deflection of muons in a magnetic field generated by superconducting air-core toroids. The field integral of the toroids ranges between 2.0 and 6.0 Tm across most of the detector. The minimum-bias trigger scintillators (MBTS) detect charged particles over $2.07 < |\eta| < 3.86$ using two hodoscopes of 12 counters positioned at $z = \pm 3.6$ m. The zero-degree calorimeters (ZDC) measure neutral particles at pseudorapidities $|\eta| \geq 8.3$ and consist of layers of alternating quartz rods and tungsten plates. A two-level trigger system [37] is used to select events. The first-level trigger (L1) is implemented in hardware and uses a subset of the detector information to reduce the accepted rate to below 100 kHz. This is followed by a software-based high-level trigger (HLT) stage that reduces the accepted event rate to 1–4 kHz depending on the data-taking conditions during Pb+Pb collisions.

3. Event selection

Data used in this analysis were recorded with the ATLAS detector in 2015 and 2018 from Pb+Pb collisions at $\sqrt{s_{NN}} = 5.02$ TeV with integrated luminosities of 0.5 nb^{-1} and 1.4 nb^{-1} , respectively. Events were selected online using a set of muon triggers that require a muon at the HLT stage with p_T larger than 3, 4, 6, or 8 GeV [37]. The muon trigger selecting $p_T > 8$ GeV sampled the full luminosity in both 2015 and 2018, while triggers with lower p_T thresholds were prescaled to reduce the overall data rate. Thus the higher-threshold triggers are utilised at a given muon p_T to sample a larger fraction of the full luminosity. The resulting sampled luminosities are 0.3 nb^{-1} , 0.6 nb^{-1} , and 1.9 nb^{-1} for muons with $4 < p_T < 6$ GeV, $6 < p_T < 8$ GeV and $p_T > 8$ GeV, respectively. The selected events are further required to satisfy offline minimum-bias Pb+Pb collision criteria to reject pile-up based on a combination of the total transverse energy measured in the FCal, denoted by ΣE_T^{FCal} , and the ZDC energy.

The centrality of each Pb+Pb event is characterised by its ΣE_T^{FCal} . For the results shown here, the minimum-bias ΣE_T^{FCal} distribution is divided into percentiles ordered from the most central (large ΣE_T^{FCal} , small impact parameter) to the most peripheral (small ΣE_T^{FCal} , large impact parameter): 0–10%, 10–20%, 20–30%, 30–40%, and 40–60%, where 0–100% corresponds to the total Pb+Pb inelastic cross section. A Monte Carlo Glauber [38] calculation is used to characterise each centrality interval [39]. The above centrality intervals have an average number of participating nucleons $\langle N_{part} \rangle = 358.8 \pm 2.3$, 264.1 ± 2.9 , 189.2 ± 2.8 , 131.4 ± 2.6 , and 70.5 ± 2.2 respectively.

Muons with $4 < p_T < 30$ GeV and $|\eta| < 2.0$ reconstructed in both the ID and the MS are selected and required to pass ‘medium’ selection requirements, detailed in Ref. [40], without any requirement on the number of TRT hits, due to the high occupancy in heavy-ion running. Candidate muons are required to be matched

¹ ATLAS uses a right-handed coordinate system with its origin at the nominal interaction point (IP) in the centre of the detector and the z -axis along the beam pipe. The x -axis points from the IP to the centre of the LHC ring, and the y -axis points upwards. Cylindrical coordinates (r, ϕ) are used in the transverse plane, ϕ being the azimuthal angle around the z -axis. The pseudorapidity is defined in terms of the polar angle θ as $\eta = -\ln \tan(\theta/2)$. Angular distance is measured in units of $\Delta R = \sqrt{(\Delta\eta)^2 + (\Delta\phi)^2}$.

with a muon reconstructed by the event trigger. Each muon is assigned a weight given by the inverse of the reconstruction and trigger efficiency for the specific muon kinematics.

The muon reconstruction and trigger efficiencies are determined using the $J/\psi \rightarrow \mu^+\mu^-$ tag-and-probe method as detailed in Ref. [40]. The muon reconstruction efficiency is factorised as the product of ID and MS reconstruction efficiencies. The ID reconstruction efficiency is obtained from Pb+Pb data directly, while the MS reconstruction efficiency is obtained both from Pb+Pb data and by overlaying Pb+Pb minimum-bias events on simulated J/ψ produced by PYTHIA 8 [41] with the CTEQ6L1 [42] parton distribution functions, using the same tag-and-probe method. The events in overlay simulations are then given weights such that the ΣE_T^{FCal} distribution matches the muon-triggered Pb+Pb data distribution. The MS reconstruction efficiency obtained from simulation is used as the central value for MS reconstruction, with additional data-to-MC scale factors applied to account for residual differences between data and overlay simulation. The same $J/\psi \rightarrow \mu^+\mu^-$ tag-and-probe method is used to determine the muon trigger efficiency. The central value of the single-muon trigger efficiency correction is obtained from simulations without overlaying Pb+Pb minimum-bias events. Additional correction factors of order 1–10% are obtained from data and applied to the selection to correct for trigger detector performance differences between data and simulation, as well as the centrality dependence of the muon trigger efficiency in Pb+Pb data.

4. Analysis procedure

The analysis follows the event-plane method for measuring flow coefficients as used in previous ATLAS measurements [7,39] and is briefly summarised here. Each Pb+Pb event has a geometric orientation of the impact parameter vector, and the event can also have a tilt relative to that due to fluctuations in the geometry of the resulting QGP. In any particular Pb+Pb collision, one can estimate the orientation, represented by the FCal-determined n^{th} -order event-plane angle Ψ_n . The azimuthal distribution of transverse energy deposited in the forward and backward rapidity FCal is used to determine the event plane. A comparison of event planes, as measured separately in the forward-rapidity FCal and the backward-rapidity FCal, enables a determination of the event-plane resolution $\text{Res}\{n\Psi_n\}$ as detailed in Ref. [39]. In each Pb+Pb centrality interval and in each muon p_T selection, the muons are divided into a finite number of intervals in $\phi - \Psi_n$, where ϕ is the azimuthal angle of the muon. As different harmonic orders are orthogonal to each other, the Fourier decomposition of the angular distribution (introduced in Eq. (1)) at a given order n can be expressed as

$$\frac{1}{N_X^\mu} \frac{dN_X^\mu}{d(n(\phi - \Psi_n))} = 1 + 2v_n^{\text{raw}} \cos(n(\phi - \Psi_n)),$$

where the v_n^{raw} are the raw flow coefficients and the N_X^μ are the extracted yields for the muons of interest. Three types of signal are considered in this measurement (X = charm, bottom, and inclusive heavy-flavour). The final v_n coefficients are obtained by correcting for the event-plane resolution: $v_n = v_n^{\text{raw}} / \text{Res}\{n\Psi_n\}$. The leading sources of background contribution in the selected muon samples are muons from decay-in-flight and punch-through of π and K (π/K background) and muons from non-heavy-flavour components such as direct quarkonia, low-mass resonances, τ -leptons and W/Z decays (labelled “light/onia background”). Other sources of background from hadronic showers and fake muons are found to be very small and are only considered in systematic uncertainties.

Similarly to previous ATLAS publications [7,33,43], different sources of muons are separated using two variables. The first is the momentum imbalance, $\rho = (p^{\text{ID}} - p^{\text{MS}})/p^{\text{ID}}$, where p^{ID} is the muon momentum measured in the ID, and p^{MS} is that measured in the MS corrected for the energy loss inside the calorimeter. Real muons have a ρ distribution peaked around zero while the π/K background has a broader ρ distribution that is shifted toward higher values. The different shapes of the ρ distribution for the π/K background and other muons enable the isolation of the π/K background muons. The analysis is repeated using the transverse momentum imbalance, as opposed to the total momentum imbalance ρ , and no difference is observed. The second variable is the transverse impact parameter, d_0 , relative to the event’s primary vertex [44]. Charm and bottom muons have different d_0 distributions due to the different decay lengths of charm and bottom hadrons.

A two-step fit in ρ and d_0 is performed in data, using ρ and d_0 line-shape templates for different sources of muons obtained from simulations. First, the yields of inclusive heavy-flavour and π/K background muons are extracted from a fit to the ρ distribution. The relative yields of light/onia background muons and inclusive heavy-flavour muons are fixed to the fractions obtained from PYTHIA 8 simulations, which are approximately 4% on average. Then, with the extracted π/K background yields fixed, a fit to the d_0 distribution is performed to determine the relative fraction of charm and bottom muons within the yield of inclusive heavy-flavour muons.

The muon ID momentum resolution in PYTHIA 8 simulations overlaid with minimum-bias Pb+Pb events is found to be worse than the resolution in Pb+Pb data. Thus, the ρ templates are obtained from simulation without Pb+Pb event overlay. The single-muon ID and MS momentum responses in the PYTHIA 8 simulation are shifted and smeared in order to match those in Pb+Pb data. The single-muon momentum shift and smearing parameters are determined by comparing the invariant mass resolution of simulated $J/\psi \rightarrow \mu^+\mu^-$ events in PYTHIA 8 with that from Pb+Pb data at different centralities. The charm and bottom muon ρ templates are determined from multijet hard-scattering pp collision events at $\sqrt{s} = 13$ TeV filtered on the presence of a generator-level muon in PYTHIA 8 with parameter values as in the A14 tune [45] and using the NNPDF23LO parton distribution functions [46]. The π/K background ρ templates are obtained from non-diffractive QCD simulations of pp collisions at $\sqrt{s} = 13$ TeV in PYTHIA 8, also with the A14 tune and NNPDF23LO parton distribution functions. The ρ templates for the light/onia background contribution are obtained from simulations of direct J/ψ in pp collisions at $\sqrt{s} = 5.02$ TeV. No differences in the template shapes were observed between simulations at $\sqrt{s} = 13$ TeV and $\sqrt{s} = 5.02$ TeV. The signal muon ρ distribution shape shows no obvious dependence on muon p_T , but is found to be broader in the endcap muon detector and in most central events due to poorer muon momentum resolution in the ID.

As the d_0 resolution is sensitive to the primary vertex position resolution, the d_0 templates are all obtained from PYTHIA 8 simulations at $\sqrt{s} = 5.02$ TeV overlaid with minimum-bias Pb+Pb events to best approximate the primary vertex resolution. The distributions of d_0 are shifted and smeared to remove residual differences between overlay simulations and Pb+Pb data. The d_0 shift and smearing parameters are found by comparing the distributions of high-quality prompt-tracks between Pb+Pb data and overlay simulations. The charm and bottom muon d_0 templates are obtained from multijet hard-scattering simulations filtered on the presence of a generator-level muon, whereas the π/K background d_0 templates are from non-diffractive QCD simulations, and the templates for light/onia background are obtained from direct J/ψ simulations. The signal muon d_0 distribution shape shows no dependence

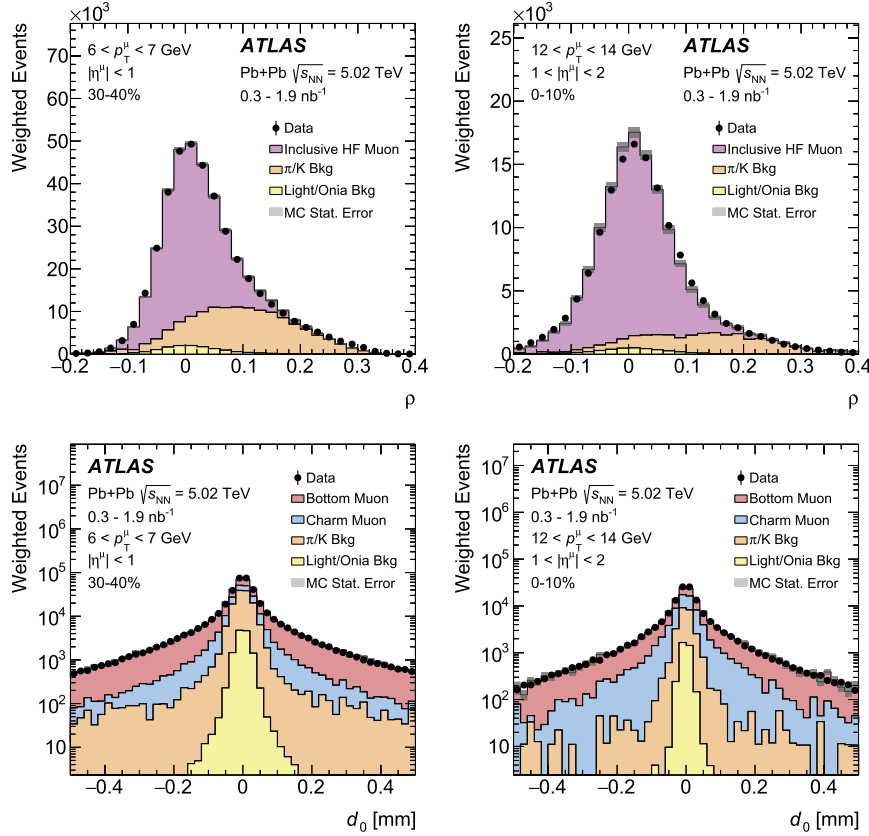


Fig. 1. Example fits to ρ (top) and d_0 (bottom) for muons with $6 < p_T < 7$ GeV and $|\eta| < 1$ in 30–40% centrality Pb+Pb collisions (left) and $12 < p_T < 14$ GeV and $1 < |\eta| < 2$ in 0–10% centrality Pb+Pb collisions (right) both integrated over $n|\phi - \Psi_n|$. Muon trigger and reconstruction efficiency corrections are applied to the data.

on muon p_T or event centrality but a moderate dependence on parent charm and bottom hadron p_T due to the strong correlation between decay length and particle velocity. Additional reweighting is applied to the charm and bottom muon signal samples to match the input charm and bottom hadron p_T spectra to those measured in Pb+Pb collisions by ALICE [11] and CMS [8,47].

The fits are performed independently in differential intervals of muon p_T , centrality, $n|\phi - \Psi_n|$ and two intervals of muon η . The two muon η intervals ($|\eta| < 1$ and $1 < |\eta| < 2$) are fitted independently to minimise residual data/MC difference in the barrel and endcap muon detectors separately, and then combined to obtain charm, bottom, and inclusive heavy-flavour muon yields in the given p_T , centrality, and $n|\phi - \Psi_n|$ intervals as reported in the results. Fluctuations in the simulation templates are incorporated in the fitting procedure. Examples of selected fits in ρ and d_0 based on simulation templates are shown in Fig. 1 for two different muon p_T selections ($6 < p_T < 7$ GeV and $12 < p_T < 14$ GeV) integrated over $n|\phi - \Psi_n|$.

The top row of Fig. 2 shows the inclusive heavy-flavour muon yield as a function of $2|\phi - \Psi_2|$ (left) and $3|\phi - \Psi_3|$ (right), and the bottom row shows the charm and bottom muon yields as a function of $2|\phi - \Psi_2|$ (left) and $3|\phi - \Psi_3|$ (right). The lines indicate the second (left) and third (right) extracted Fourier harmonics from which the v_2^{aw} and v_3^{aw} coefficients are extracted.

5. Systematic uncertainties

Systematic uncertainties are presented for different categories covering each step of the analysis procedure: 1) muon efficiency; 2) ρ fit; 3) d_0 fit; 4) light/onia background; 5) other background; 6) ρ – d_0 correlation; 7) event-plane resolution; and 8) jet bias. Table 1 summarises the contributions from different sources of sys-

tematic uncertainty to the final flow-coefficient results. Systematic uncertainties from all sources are summed in quadrature to determine the total uncertainty.

The systematic uncertainties from the MS reconstruction efficiency and muon trigger efficiency corrections are dominated by the uncertainty in determining the data-to-MC scale factor. The scale factor uncertainties are evaluated following the procedure from previous ATLAS measurements [40] including variations in the tag-and-probe efficiency extraction method, object-matching resolution, and purity of the sample. The systematic uncertainty in the muon trigger efficiency also includes the determination of the centrality-dependent correction factors. The uncertainty on the flow coefficients resulting from uncertainties in the muon ID reconstruction efficiency is evaluated by comparing the results with and without the ID efficiency correction, as the ID efficiency is approximately 99% for all centralities. The muon efficiency systematic uncertainties are correlated between the resulting charm and bottom muon results.

The systematic uncertainty of the ρ fit is due to the uncertainty in the shifts and smearing parameters for single-muon momentum response in simulation, which is evaluated by comparing the nominal results with those 1) without any shifts or smearing, 2) only applying shifts and smearing to the signal muons, and 3) incorporating additional smearing of the background ρ distributions in simulation to match data distributions in the background-enriched region ($\rho > 0.2$). The changes resulting from these variations are combined in quadrature. The combined uncertainty from the ρ fit is 1%–10% for the charm and bottom muon results, depending on the muon p_T and η , but without dependence on centrality. The relative systematic variations are found to be the largest at low p_T and large η . The ρ fit systematic uncertainties are correlated between the resulting charm and bottom muon results.

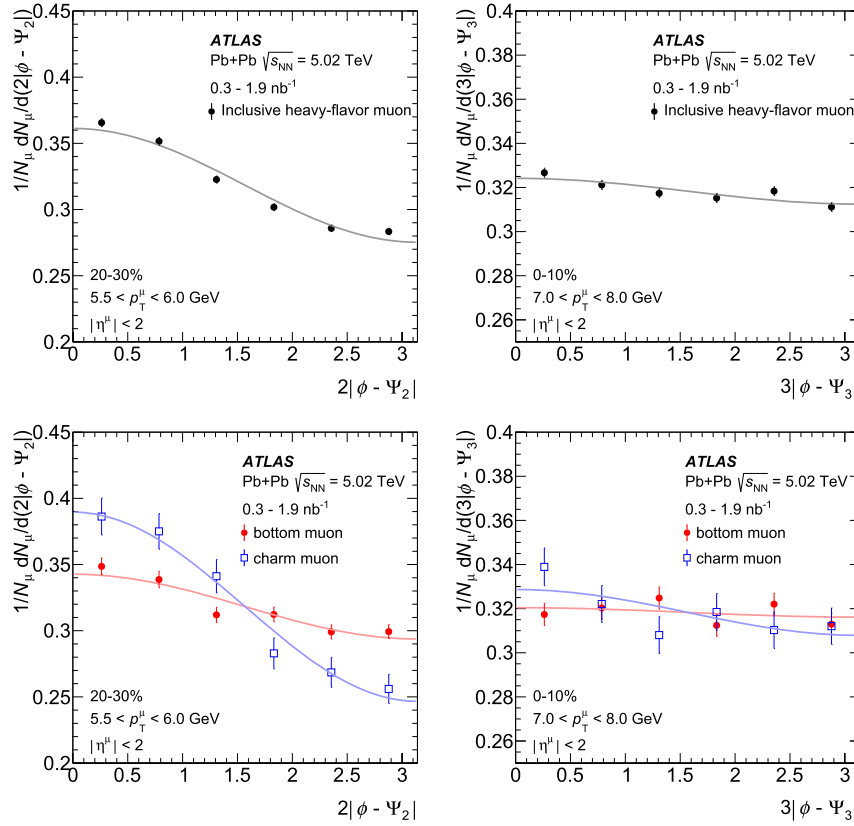


Fig. 2. Examples of Fourier decomposition of inclusive heavy-flavour muon yields (top) and bottom/charm muon yields (bottom) in Pb+Pb collisions at $\sqrt{s_{NN}} = 5.02$ TeV as a function of $2|\phi - \Psi_2|$ (left) and $3|\phi - \Psi_3|$ (right) for two selected intervals in muon p_T and centrality. The inclusive heavy-flavour muon yields are obtained from ρ template fits, while the bottom and charm muon yields are further separated using d_0 fits. In all cases the error bars on data indicate the statistical uncertainties obtained from the ρ or d_0 fit. The lines indicate the extracted second (left) and third (right) Fourier harmonics.

Table 1

Summary of the typical sizes of the absolute systematic uncertainties of all categories for the flow coefficient results. The d_0 related systematic uncertainties are not relevant for the heavy-flavour inclusive flow measurements as the d_0 fit is not utilised for these results. Systematic uncertainties from the event-plane resolution and jet bias are negligible and not included in the final uncertainties, and therefore are not shown in the table. The “<” symbol indicates the provided values are the maximum systematic variation for a given category.

Category	Inclusive heavy-flavour muon v_2 (v_3)	Charm muon v_2 (v_3)	Bottom muon v_2 (v_3)
Muon efficiency	< 0.0002 (0.0006)	< 0.006 (0.001)	< 0.001 (0.001)
ρ fit	< 0.004 (0.006)	< 0.009 (0.01)	< 0.005 (0.003)
d_0 fit	N/A	< 0.02 (0.03)	< 0.01 (0.01)
Light/onion bkg	< 0.004 (0.002)	< 0.02 (0.01)	< 0.008 (0.004)
Other bkg	< 0.000001 (0.000001)	< 0.002 (0.004)	< 0.001 (0.0004)
ρ - d_0 correlation	N/A	< 0.01 (0.004)	< 0.007 (0.005)

The uncertainty in the d_0 template shift and smearing parameters is tested by comparing results when determining the parameters using 2018 data (as in the nominal results) with results when using the 2015 Pb+Pb data to determine the parameters, which covers the slightly different detector alignment between the two data sets. Sensitivity to the charm and bottom hadron p_T spectra reweighting in simulation is covered by a variation in which the p_T spectra are reweighted to agree with those from PYTHIA 8 simulations without any modification due to QGP. The variations in the results due to d_0 template shift and smearing and p_T spectra reweighting are considered to be uncorrelated and are combined in quadrature, and the combined systematic uncertainty is 1%–20% for the charm and bottom muon results, depending on muon p_T and centrality. The relative systematic variations are found to be the largest at high p_T and in more peripheral events. The d_0 fit systematic uncertainties are anti-correlated between the resulting charm and bottom muon results.

The magnitude of the light/onion contribution is held at a fixed fraction relative to the inclusive heavy-flavour muon contribution, based on the PYTHIA 8 MC sample. The analysis is repeated to study this choice, first ignoring the light/onion contribution and then fixing it to twice the fraction predicted by PYTHIA 8. As is shown in Ref. [48], PYTHIA overestimates prompt quarkonium production at the LHC, and thus these variations of the light/onion contribution are large enough to not underestimate the uncertainty. Each nominal result is assigned a systematic uncertainty equal to the larger of the changes from the two variations. For the nominal results, light/onion muons are assumed to have the same v_2 and v_3 as the inclusive heavy-flavour muons. The analysis is repeated with variations assuming light/onion muons have zero flow coefficients or double the inclusive heavy-flavour muon flow coefficients. The larger of the resulting changes is assigned as the systematic uncertainty. The light/onion systematic uncertainties are anti-correlated between the resulting charm and bottom muon results.

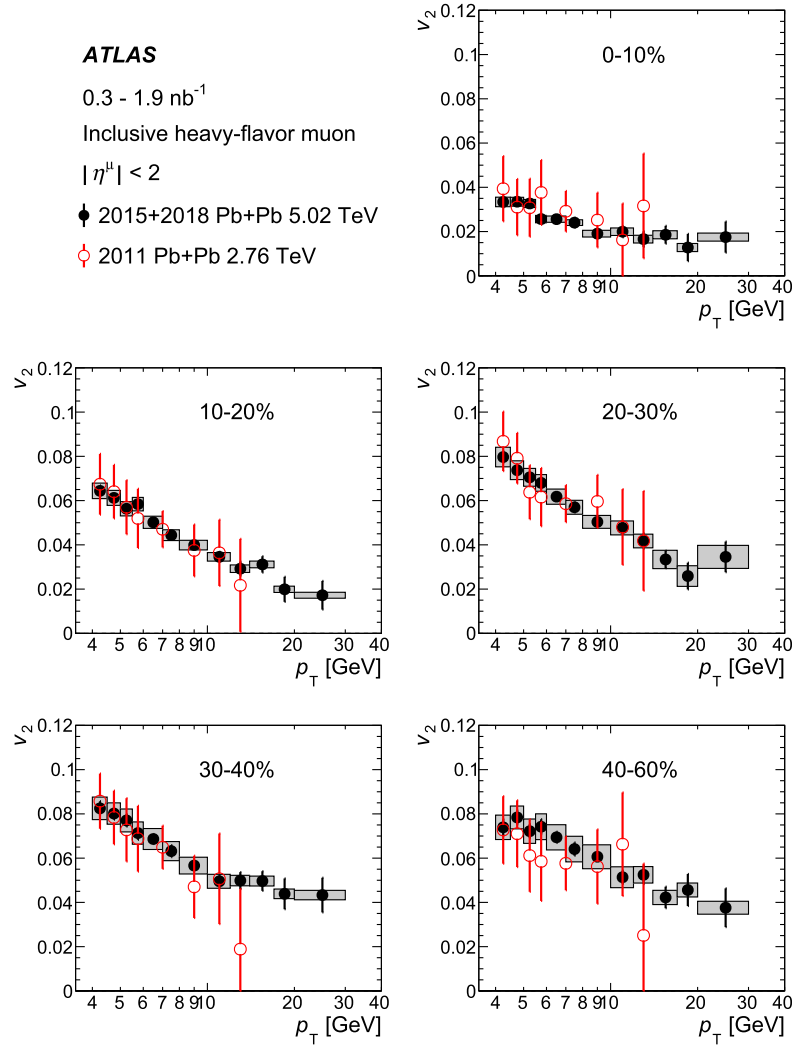


Fig. 3. Inclusive heavy-flavour muon v_2 as a function of p_T in the combined 2015 and 2018 $\sqrt{s_{NN}} = 5.02$ TeV Pb+Pb data compared with the results in the $\sqrt{s_{NN}} = 2.76$ TeV Pb+Pb data [7]. Statistical uncertainties are shown as vertical lines and systematic uncertainties as boxes for the $\sqrt{s_{NN}} = 5.02$ TeV results. For better visibility the statistical and systematic uncertainties of the $\sqrt{s_{NN}} = 2.76$ TeV data are combined in quadrature and shown as vertical lines. Each panel represents a different centrality interval.

The contributions of hadronic showers are ignored in the nominal analysis. They were included in the analysis based on ρ and d_0 templates from the PYTHIA 8 simulation with a fixed relative fraction of a few percent also obtained from PYTHIA 8 simulation. The deviation from the nominal result is found to be negligible for the inclusive heavy-flavour muon flow coefficients, and approximately 8% at low p_T (< 8 GeV) and less than 1% at high p_T (> 12 GeV) for charm and bottom muon flow coefficients.

All muons are assumed to have independent ρ and d_0 distributions in the nominal results, which is only true for signal muons. To test the sensitivity to this assumption, d_0 fits in data are repeated with a requirement of $\rho < 0.1$ on the sample, thus significantly reducing the background contribution. The difference between results with and without the restriction on ρ is assigned as a systematic uncertainty to cover the systematic effect of ignoring any correlation between ρ and d_0 for background muons.

The systematic uncertainty associated with the event-plane angle resolution is evaluated by measuring the event-plane resolution in two subregions of the FCal ($3.2 < |\eta| < 4.0$ and $4.0 < |\eta| < 4.8$), following a previous ATLAS flow analysis [39]. The systematic uncertainties are evaluated independently for Ψ_2 and Ψ_3 . The maximum difference between these two variations and the nominal results is considered as a systematic uncertainty. The uncertainty associated with the event-plane angle resolution is found to be

negligible compared to other systematic uncertainties, and thus is not included in the results.

The charm and bottom muons are often produced with a recoil jet. The orientation of Ψ_n could be biased to align with the signal muon if the recoil jet reaches the FCal [7]. The magnitude of this bias in muon v_2 and v_3 is studied with PYTHIA generator-level muon flow in samples overlaid with Pb+Pb data. The bias is found to be 0.3%–0.4% for v_2 and v_3 , and it is larger in peripheral events than in more-central events. This small bias is negligible and is not included as a systematic uncertainty.

6. Results

Fig. 3 shows the inclusive heavy-flavour muon elliptic flow coefficient v_2 as a function of p_T in the $\sqrt{s_{NN}} = 5.02$ TeV Pb+Pb data. Each panel corresponds to a different Pb+Pb centrality interval. The v_2 results decrease steadily with p_T over the entire p_T range and in all centrality intervals. The overall magnitude of v_2 is smaller in the most central 0–10% selection, as expected since the corresponding smaller impact parameter Pb+Pb collisions have smaller initial geometric ellipticity.

Fig. 4 shows the inclusive heavy-flavour muon triangular flow coefficient v_3 as a function of p_T in the $\sqrt{s_{NN}} = 5.02$ TeV Pb+Pb data. Each panel corresponds to a different Pb+Pb centrality in-

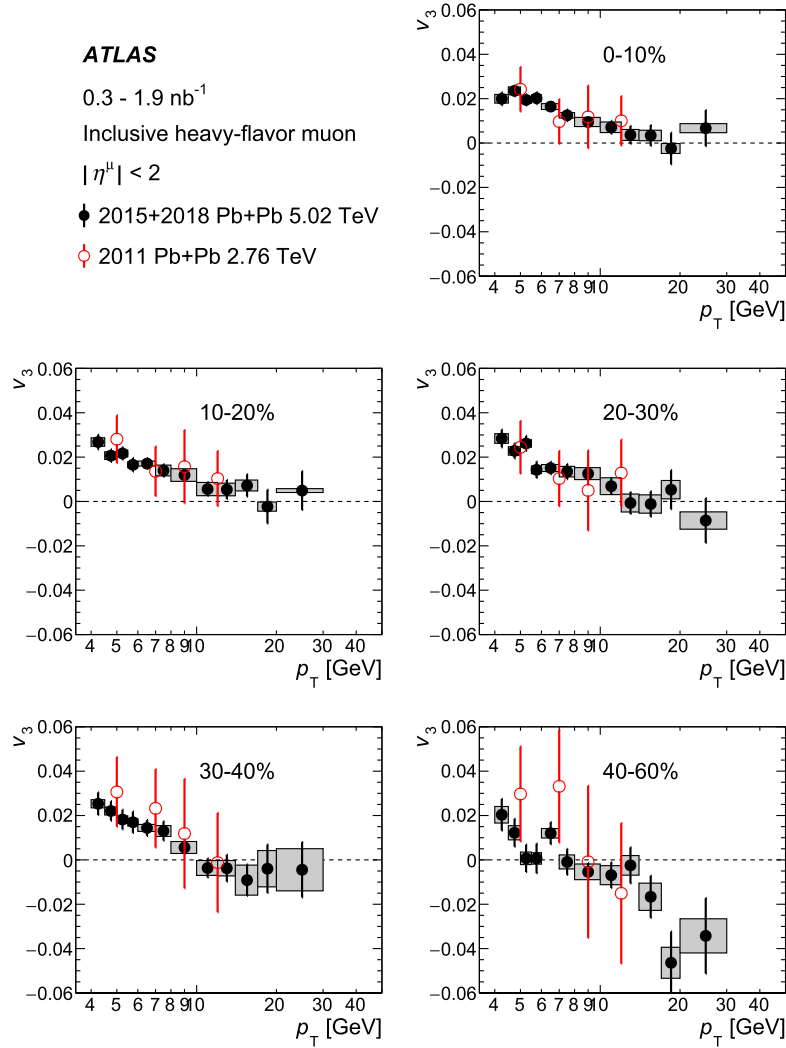


Fig. 4. Inclusive heavy-flavour muon v_3 as a function of p_T in the combined 2015 and 2018 $\sqrt{s_{NN}} = 5.02$ TeV Pb+Pb data compared with the results in the $\sqrt{s_{NN}} = 2.76$ TeV Pb+Pb data [7]. Statistical uncertainties are shown as vertical lines and systematic uncertainties as boxes for the $\sqrt{s_{NN}} = 5.02$ TeV results. For better visibility the statistical and systematic uncertainties of the $\sqrt{s_{NN}} = 2.76$ TeV data are combined in quadrature and shown as vertical lines. Each panel represents a different centrality interval.

terval. The v_3 results decrease steadily with p_T over the entire p_T range in all centrality intervals within statistical and systematic uncertainties. The overall magnitude of v_3 is quite similar in all centrality intervals, as expected since triangular deformations of the initial geometry are primarily the result of fluctuations and are generally unrelated to any intrinsic geometry from the colliding nuclei [49].

Each panel of Figs. 3 and 4 also presents previous ATLAS results from $\sqrt{s_{NN}} = 2.76$ TeV Pb+Pb data [7]. Compared to the earlier result, the present $\sqrt{s_{NN}} = 5.02$ TeV results significantly improve the statistical precision of the measurements and extend the p_T range. The $\sqrt{s_{NN}} = 5.02$ TeV and $\sqrt{s_{NN}} = 2.76$ TeV Pb+Pb data inclusive heavy-flavour muon v_2 and v_3 coefficients are consistent with each other within uncertainties. Indeed, according to hydrodynamical models, no significant differences are expected between Pb+Pb collisions at the two different energies [50]. Thus the observed consistency between $\sqrt{s_{NN}} = 2.76$ TeV and $\sqrt{s_{NN}} = 5.02$ TeV data is in agreement with expectations. The inclusive charged-particle flow coefficients are also observed to be nearly identical at the two collision energies [39].

Fig. 5 shows the separated charm and bottom muon v_2 as a function of p_T , with each panel presenting a different Pb+Pb centrality interval. The charm and bottom flow coefficients are extracted only up to $p_T = 20$ GeV, since above that transverse mo-

mentum range the inclusive heavy-flavour v_2 values are small and the charm-to-bottom separation procedure becomes sensitive to fluctuations in data and yields unstable results. The results indicate a non-zero v_2 for both the charm and bottom muons, with substantially larger elliptic flow coefficients for charm muons. The statistical and systematic uncertainties have a significant contribution that is anti-correlated between the charm and bottom v_2 , i.e. an upward fluctuation in the charm v_2 in a particular p_T bin will be correlated with a downward fluctuation in the bottom v_2 in the same bin and vice versa. For $p_T < 14$ GeV, both charm and bottom muon v_2 increase from central to mid-central events, reaching maximum between 20% and 40% centrality. Over the range of $p_T > 14$ GeV, the charm and bottom muon v_2 show no obvious centrality dependence with larger uncertainties.

Qualitatively, the charm and bottom v_2 ordering matches theoretical expectations where the heavier bottom quarks have a smaller modification to their initial momentum trajectories due to their larger masses. Light quarks and heavy quarks can lose energy in traversing the QGP via induced gluon radiation [51]; however, heavy quarks with momentum less than or approximately equal to the quark mass ($p \lesssim m$) radiate less than light quarks due to a suppression of radiation at small angles relative to the quark direction, referred to as the ‘dead-cone’ effect [5]. Thus, at high $p_T \gg m$, all quark flavors should lose comparable energy in the

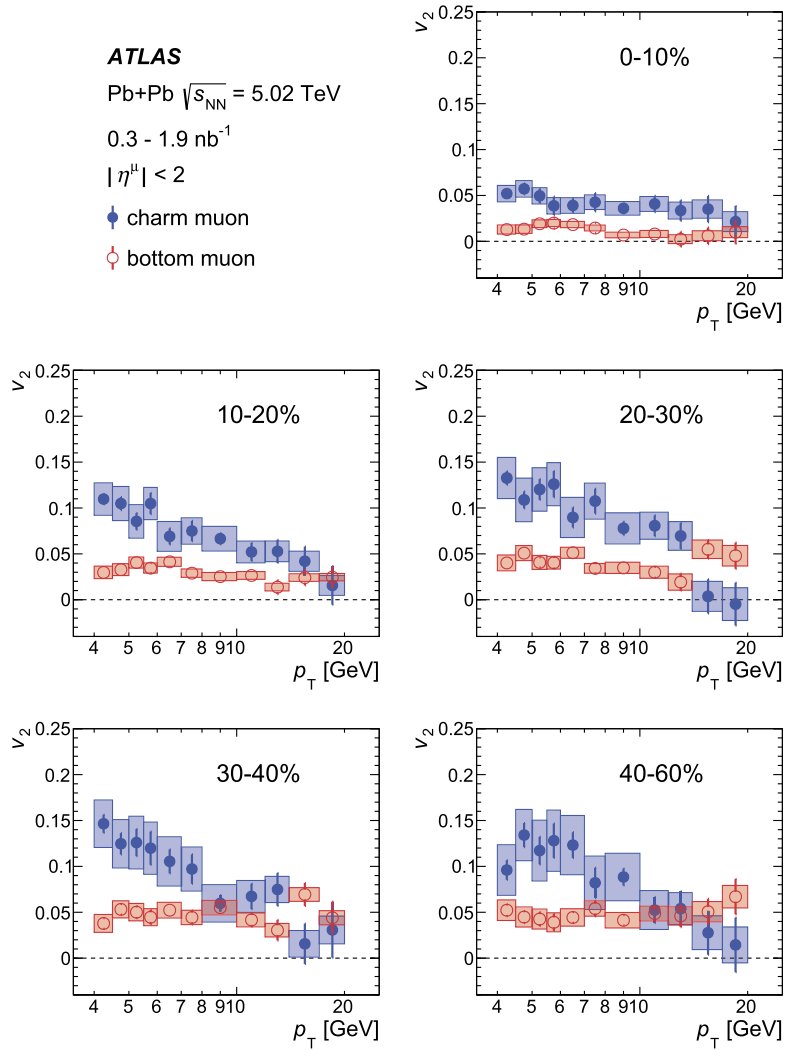


Fig. 5. Charm and bottom muon v_2 as a function of p_T in the combined 2015 and 2018 $\sqrt{s_{NN}} = 5.02$ TeV Pb+Pb data. Statistical uncertainties are shown as vertical lines and systematic uncertainties as boxes for charm and bottom muons. The charm and bottom uncertainties are partially anti-correlated. Each panel presents a different centrality interval.

QGP, while at lower p_T there should be a hierarchy with light quarks losing the most energy, then charm quarks, and finally bottom quarks losing the least energy. Thus the heavier bottom quarks with $p_T \lesssim 20 - 30$ GeV are expected to lose less energy in the QGP and thus have a smaller azimuthal anisotropy.

Fig. 6 shows the separated charm and bottom muon v_3 as a function of p_T , with each panel presenting a different Pb+Pb centrality interval. The charm muons show significant non-zero v_3 values, which are independent of centrality. The bottom muons have v_3 values that are significantly below that of charm muons at all p_T and in all centrality intervals.

Fig. 7 shows the results for v_2 versus p_T , from Fig. 5, compared with theoretical calculations: DREENA-B from Ref. [30], and DAB-MOD from Refs. [29,52] for charm and bottom decay muons in the Pb+Pb 0–10% (left) and 40–60% (right) centrality intervals. The DREENA-B calculation includes radiative and collisional energy loss of the heavy quarks traversing the QGP, the latter modelled via a $1 + 1D$ Bjorken expansion [53]. The DREENA-B theoretical uncertainties reflect the range of magnetic to electric screening masses as constrained by non-perturbative calculations [53]. The predicted D meson v_2 is higher than the B meson v_2 , with the two converging at $p_T \approx 25$ GeV as expected when the p_T is much larger than the charm and bottom quark masses. Using PYTHIA 8 for decay kinematics, the charm muon and bottom muon v_2 results are

calculated and shown. The predominant effect in going from the parent meson $v_2(p_T)$ to the daughter muon $v_2(p_T)$ is a shift downward in p_T . The predictions are in reasonable agreement with the experimental data, although they overestimate the v_2 at high p_T of bottom muons in central events. The DAB-MOD framework includes calculations with only Langevin drag and diffusion contributions. The curves shown here are obtained with TRENTO geometric initial conditions [54], heavy-quark Langevin dynamics with the Moore and Teaney parameterisation [19], and coupling values for charm (bottom) of $D/2\pi T = 2.23$ (2.79), where D is the spatial diffusion coefficient and T is the temperature. The decoupling temperature of heavy quarks from the medium is $T = 160$ MeV and both coalescence and fragmentation are implemented for hadronisation. The DAB-MOD predictions with only Langevin dynamics are roughly a factor of three (two) lower for charm (bottom) muons compared with DREENA-B. Additional energy loss contributions to DAB-MOD, not included here, tend to increase the high p_T anisotropies. At lower p_T , the DREENA-B v_2 results rise significantly. A key component of these calculations is the modelling of the QGP transverse

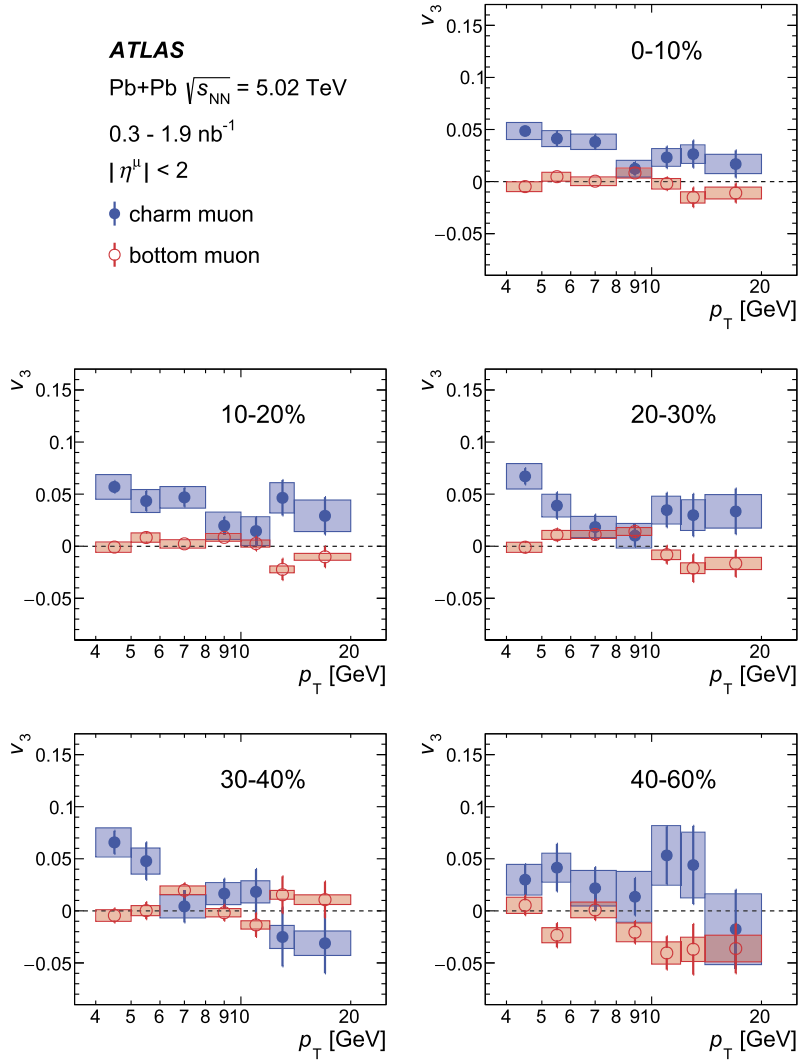


Fig. 6. Charm and bottom muon v_3 as a function of p_T in the combined 2015 and 2018 $\sqrt{s_{NN}} = 5.02$ TeV Pb+Pb data. Statistical uncertainties are shown as vertical lines and systematic uncertainties as boxes for charm and bottom muons. The charm and bottom uncertainties are partially anti-correlated. Each panel presents a different centrality interval.

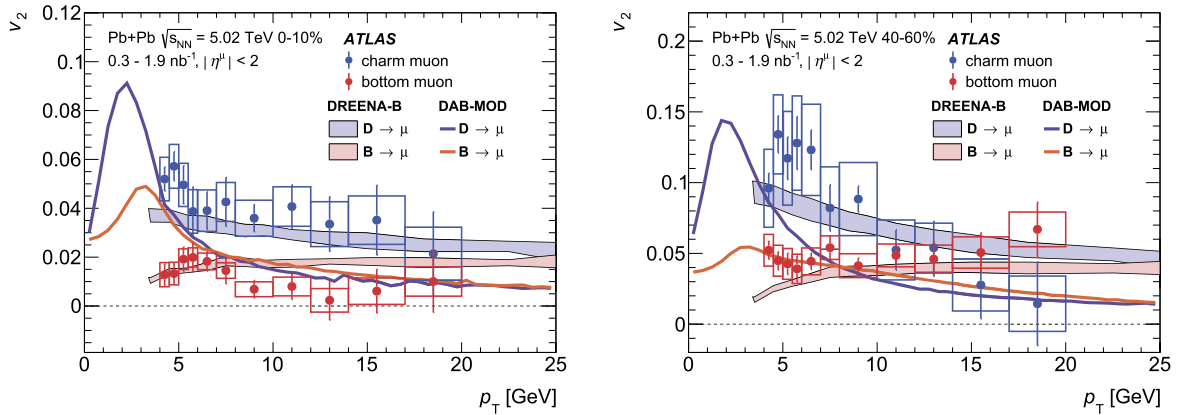


Fig. 7. Charm and bottom muon v_2 as a function of p_T in the $\sqrt{s_{NN}} = 5.02$ TeV Pb+Pb data for the 0-10% (left) and 40-60% (right) centrality interval, compared with theoretical predictions based on DREENA-B [30] and DAB-MOD [29,52] in the same centrality intervals for charm and bottom muon v_2 . For the data, statistical uncertainties are shown as vertical lines and systematic uncertainties as boxes. The charm and bottom uncertainties are partially anti-correlated.

expansion, and thus it will be instructive in the future to compare the calculations with a common QGP model to test whether the differences arise from the QGP modelling or the energy-loss implementation.

7. Conclusion

In summary, a measurement of elliptic and triangular flow coefficients for heavy-flavour decay muons in Pb+Pb collisions at

$\sqrt{s_{NN}} = 5.02$ TeV is presented, including a separation between charm and bottom contributions. The measurement uses a combined 2015 and 2018 data set corresponding to a total integrated luminosity of up to 1.9 nb^{-1} recorded by the ATLAS experiment at the LHC. The inclusive heavy-flavour muon v_2 and v_3 values measured in $4 < p_T < 30$ GeV are observed to decrease with p_T for all centrality intervals. The v_2 and v_3 values are consistent within uncertainties with previous Pb+Pb measurements at $\sqrt{s_{NN}} = 2.76$ TeV. Further separating the inclusive heavy-flavour muons into charm and bottom muons reveals a significantly larger v_2 and v_3 for charm muons than for bottom muons. The results indicate that while both the charm and bottom quarks have their trajectories and momenta modified when traversing the QGP, the effect is stronger for the charm quarks. At fixed p_T , the charm and bottom muon v_2 values decrease from 40-60% to 0-10% centrality intervals as observed in charged hadron elliptic-flow measurements [55]. Theoretical calculations have a similar qualitative trend with smaller flow coefficients for muons from decays of the heavier bottom quarks. The results can significantly discriminate between models of heavy-quark energy loss and constrain heavy-quark transport coefficients in the QGP.

Declaration of competing interest

The authors declare that they have no known competing financial interests or personal relationships that could have appeared to influence the work reported in this paper.

Acknowledgements

We thank CERN for the very successful operation of the LHC, as well as the support staff from our institutions without whom ATLAS could not be operated efficiently.

We acknowledge the support of ANPCyT, Argentina; YerPhI, Armenia; ARC, Australia; BMWFW and FWF, Austria; ANAS, Azerbaijan; SSTC, Belarus; CNPq and FAPESP, Brazil; NSERC, NRC and CFI, Canada; CERN; CONICYT, Chile; CAS, MOST and NSFC, China; COLCIENCIAS, Colombia; MSMT CR, MPO CR and VSC CR, Czech Republic; DNRF and DNSRC, Denmark; IN2P3-CNRS and CEA-DRF/IRFU, France; SRNSFG, Georgia; BMBF, HGF and MPG, Germany; GSRF, Greece; RGC and Hong Kong SAR, China; ISF and Benoziyo Center, Israel; INFN, Italy; MEXT and JSPS, Japan; CNRST, Morocco; NWO, Netherlands; RCN, Norway; MNiSW and NCN, Poland; FCT, Portugal; MNE/IFA, Romania; MES of Russia and NRC KI, Russia Federation; JINR; MESTD, Serbia; MSSR, Slovakia; ARRS and MIZŠ, Slovenia; DST/NRF, South Africa; MINECO, Spain; SRC and Wallenberg Foundation, Sweden; SERI, SNSF and Cantons of Bern and Geneva, Switzerland; MOST, Taiwan; TAEK, Turkey; STFC, United Kingdom; DOE and NSF, United States of America. In addition, individual groups and members have received support from BCKDF, CANARIE, Compute Canada and CRC, Canada; ERC, ERDF, Horizon 2020, Marie Skłodowska-Curie Actions and COST, European Union; Investissements d'Avenir Labex, Investissements d'Avenir Idex and ANR, France; DFG and AvH Foundation, Germany; Herakleitos, Thales and Aristeia programmes co-financed by EU-ESF and the Greek NSRF, Greece; BSF-NSF and GIF, Israel; CERCA Programme Generalitat de Catalunya and PROMETEO Programme Generalitat Valenciana, Spain; Göran Gustafssons Stiftelse, Sweden; The Royal Society and Leverhulme Trust, United Kingdom.

The crucial computing support from all WLCG partners is acknowledged gratefully, in particular from CERN, the ATLAS Tier-1 facilities at TRIUMF (Canada), NDGF (Denmark, Norway, Sweden), CC-IN2P3 (France), KIT/GridKA (Germany), INFN-CNAF (Italy), NL-T1 (Netherlands), PIC (Spain), ASGC (Taiwan), RAL (UK) and BNL (USA), the Tier-2 facilities worldwide and large non-WLCG resource

providers. Major contributors of computing resources are listed in Ref. [56].

References

- [1] P. Romatschke, U. Romatschke, *Relativistic Fluid Dynamics in and Out of Equilibrium*, Cambridge Monographs on Mathematical Physics, Cambridge University Press, 2019, arXiv:1712.05815 [nucl-th].
- [2] U. Heinz, R. Snellings, Collective flow and viscosity in relativistic heavy-ion collisions, *Annu. Rev. Nucl. Part. Sci.* 63 (2013) 123, arXiv:1301.2826 [nucl-th].
- [3] S. Voloshin, Y. Zhang, Flow study in relativistic nuclear collisions by Fourier expansion of azimuthal particle distributions, *Z. Phys. C* 70 (1996) 665, arXiv:hep-ph/9407282 [hep-ph].
- [4] M. Habich, J.L. Nagle, P. Romatschke, Particle spectra and HBT radii for simulated central nuclear collisions of C + C, Al + Al, Cu + Cu, Au + Au, and Pb + Pb from $\sqrt{s} = 62.4\text{--}2760$ GeV, *Eur. Phys. J. C* 75 (2015) 15, arXiv:1409.0040 [nucl-th].
- [5] Y.L. Dokshitzer, D.E. Kharzeev, Heavy quark colorimetry of QCD matter, *Phys. Lett. B* 519 (2001) 199, arXiv:hep-ph/0106202 [hep-ph].
- [6] S. Batoulis, S. Kelly, M. Gyulassy, J.L. Nagle, Does the charm flow at RHIC?, *Phys. Lett. B* 557 (2003) 26, arXiv:nucl-th/0212068 [nucl-th].
- [7] ATLAS Collaboration, Measurement of the suppression and azimuthal anisotropy of muons from heavy-flavor decays in Pb+Pb collisions at $\sqrt{s_{NN}} = 2.76$ TeV with the ATLAS detector, *Phys. Rev. C* 98 (2018) 044905, arXiv:1805.05220 [hep-ex].
- [8] CMS Collaboration, Nuclear modification factor of D^0 mesons in PbPb collisions at $\sqrt{s_{NN}} = 5.02$ TeV, *Phys. Lett. B* 782 (2018) 474, arXiv:1708.04962 [hep-ex].
- [9] CMS Collaboration, Studies of beauty suppression via nonprompt D^0 mesons in PbPb collisions at $\sqrt{s_{NN}} = 5.02$ TeV, *Phys. Rev. Lett.* 123 (2019) 022001, arXiv:1810.11102 [hep-ex].
- [10] CMS Collaboration, Measurement of B^\pm meson nuclear modification factor in PbPb collisions at $\sqrt{s_{NN}} = 5.02$ TeV, *Phys. Rev. Lett.* 119 (2017) 152301, arXiv:1705.04727 [hep-ex].
- [11] ALICE Collaboration, Measurement of D^0 , D^+ , D^{*+} and D_s^+ production in Pb-Pb collisions at $\sqrt{s_{NN}} = 5.02$ TeV, *J. High Energy Phys.* 10 (2018) 174, arXiv:1804.09083 [nucl-ex].
- [12] STAR Collaboration, J. Adam, et al., Centrality and transverse momentum dependence of D^0 -meson production at mid-rapidity in Au+Au collisions at $\sqrt{s_{NN}} = 200$ GeV, *Phys. Rev. C* 99 (2019) 034908, arXiv:1812.10224 [nucl-ex].
- [13] ALICE Collaboration, D -meson azimuthal anisotropy in mid-central Pb-Pb collisions at $\sqrt{s_{NN}} = 5.02$ TeV, *Phys. Rev. Lett.* 120 (2018) 102301, arXiv:1707.01005 [nucl-ex].
- [14] CMS Collaboration, Measurement of prompt D^0 meson azimuthal anisotropy in Pb-Pb collisions at $\sqrt{s_{NN}} = 5.02$ TeV, *Phys. Rev. Lett.* 120 (2018) 202301, arXiv:1708.03497 [hep-ex].
- [15] ALICE Collaboration, Elliptic flow of electrons from heavy-flavour hadron decays at mid-rapidity in Pb-Pb collisions at $\sqrt{s_{NN}} = 2.76$ TeV, *J. High Energy Phys.* 09 (2016) 028, arXiv:1606.00321 [nucl-ex].
- [16] R. Averbeck, Heavy-flavor production in heavy-ion collisions and implications for the properties of hot QCD matter, *Prog. Part. Nucl. Phys.* 70 (2013) 159, arXiv:1505.03828 [nucl-ex].
- [17] X. Dong, Y.-J. Lee, R. Rapp, Open heavy-flavor production in heavy-ion collisions, *Annu. Rev. Nucl. Part. Sci.* 69 (2019) 417, arXiv:1903.07709 [nucl-ex].
- [18] A. Andronic, et al., Heavy-flavour and quarkonium production in the LHC era: from proton-proton to heavy-ion collisions, *Eur. Phys. J. C* 76 (2016) 107, arXiv:1506.03981 [nucl-ex].
- [19] G.D. Moore, D. Teaney, How much do heavy quarks thermalize in a heavy ion collision?, *Phys. Rev. C* 71 (2005) 064904, arXiv:hep-ph/0412346 [hep-ph].
- [20] S. Cao, et al., Toward the determination of heavy-quark transport coefficients in quark-gluon plasma, *Phys. Rev. C* 99 (2019) 054907, arXiv:1809.07894 [nucl-th].
- [21] R. Rapp, et al., Extraction of heavy-flavor transport coefficients in QCD matter, *Nucl. Phys. A* 979 (2018) 21, arXiv:1803.03824 [nucl-th].
- [22] M. He, R.J. Fries, R. Rapp, D_s meson as a quantitative probe of diffusion and hadronization in nuclear collisions, *Phys. Rev. Lett.* 110 (2013) 112301, arXiv:1204.4442 [nucl-th].
- [23] W. Alberico, et al., Heavy-flavour spectra in high energy nucleus-nucleus collisions, *Eur. Phys. J. C* 71 (2011) 1666, arXiv:1101.6008 [hep-ph].
- [24] J. Uphoff, O. Fochler, Z. Xu, C. Greiner, Elliptic flow and energy loss of heavy quarks in ultrarelativistic heavy ion collisions, *Phys. Rev. C* 84 (2011) 024908, arXiv:1104.2295 [hep-ph].
- [25] P.B. Gossiaux, R. Bierkandt, J. Aichelin, Tomography of quark gluon plasma at energies available at the BNL relativistic heavy ion collider (RHIC) and the CERN large hadron collider (LHC), *Phys. Rev. C* 79 (2009) 044906, arXiv:0901.0946 [hep-ph].
- [26] B. Zhang, L.-W. Chen, C.-M. Ko, Charm elliptic flow at RHIC, *Phys. Rev. C* 72 (2005) 024906, arXiv:nucl-th/0502056 [nucl-th].
- [27] S. Wicks, W. Horowitz, M. Djordjevic, M. Gyulassy, Elastic, inelastic, and path length fluctuations in jet tomography, *Nucl. Phys. A* 784 (2007) 426, arXiv:nucl-th/0512076 [nucl-th].

- [28] M. He, R.J. Fries, R. Rapp, Heavy flavor at the large hadron collider in a strong coupling approach, *Phys. Lett. B* 735 (2014) 445, arXiv:1401.3817 [nucl-th].
- [29] R. Katz, C.A.G. Prado, J. Noronha-Hostler, J. Noronha, A.A.P. Suaide, DAB-MOD sensitivity study of heavy flavor R_{AA} and azimuthal anisotropies based on beam energy, initial conditions, hadronization, and suppression mechanisms, arXiv:1906.10768 [nucl-th], 2019.
- [30] D. Zigic, I. Salom, J. Auvinen, M. Djordjevic, M. Djordjevic, DREENA-B framework: first predictions of R_{AA} and v_2 within dynamical energy loss formalism in evolving QCD medium, *Phys. Lett. B* 791 (2019) 236, arXiv:1805.04786 [nucl-th].
- [31] W. Ke, Y. Xu, S.A. Bass, Linearized Boltzmann-Langevin model for heavy quark transport in hot and dense QCD matter, *Phys. Rev. C* 98 (2018) 064901, arXiv:1806.08848 [nucl-th].
- [32] ALICE Collaboration, Elliptic flow of muons from heavy-flavour hadron decays at forward rapidity in PbPb collisions at $\sqrt{s_{NN}} = 2.76$ TeV, *Phys. Lett. B* 753 (2016) 41, arXiv:1507.03134 [nucl-ex].
- [33] ATLAS Collaboration, Measurement of azimuthal anisotropy of muons from charm and bottom hadrons in pp collisions at $\sqrt{s} = 13$ TeV with the ATLAS detector, *Phys. Rev. Lett.* 124 (2020) 082301, arXiv:1909.01650 [hep-ex].
- [34] ATLAS Collaboration, The ATLAS experiment at the CERN large hadron collider, *J. Instrum.* 3 (2008) S08003.
- [35] ATLAS Collaboration, ATLAS insertable B-layer technical design report, ATLAS-TDR-19, <https://cds.cern.ch/record/1291633>, 2010, Addendum: ATLAS-TDR-19-ADD-1, <https://cds.cern.ch/record/1451888>, 2012.
- [36] B. Abbott, et al., Production and integration of the ATLAS insertable B-layer, *J. Instrum.* 13 (2018) T05008, arXiv:1803.00844 [physics.ins-det].
- [37] ATLAS Collaboration, Performance of the ATLAS trigger system in 2015, *Eur. Phys. J. C* 77 (2017) 317, arXiv:1611.09661 [hep-ex].
- [38] M.L. Miller, K. Reygers, S.J. Sanders, P. Steinberg, Glauber modeling in high energy nuclear collisions, *Annu. Rev. Nucl. Part. Sci.* 57 (2007) 205, arXiv:nucl-ex/0701025 [nucl-ex].
- [39] ATLAS Collaboration, Measurement of the azimuthal anisotropy of charged particles produced in $\sqrt{s_{NN}} = 5.02$ TeV Pb+Pb collisions with the ATLAS detector, *Eur. Phys. J. C* 78 (2018) 997, arXiv:1808.03951 [hep-ex].
- [40] ATLAS Collaboration, Muon reconstruction performance of the ATLAS detector in proton-proton collision data at $\sqrt{s} = 13$ TeV, *Eur. Phys. J. C* 76 (2016) 292, arXiv:1603.05598 [hep-ex].
- [41] T. Sjöstrand, et al., An introduction to PYTHIA 8.2, *Comput. Phys. Commun.* 191 (2015) 159, arXiv:1410.3012 [hep-ph].
- [42] J. Pumplin, et al., New generation of parton distributions with uncertainties from global QCD analysis, *J. High Energy Phys.* 07 (2002) 012, arXiv:hep-ph/0201195.
- [43] ATLAS Collaboration, Measurements of the electron and muon inclusive cross-sections in proton-proton collisions at $\sqrt{s} = 7$ TeV with the ATLAS detector, *Phys. Lett. B* 707 (2012) 438, arXiv:1109.0525 [hep-ex].
- [44] ATLAS Collaboration, Vertex reconstruction performance of the ATLAS detector at $\sqrt{s} = 13$ TeV, ATL-PHYS-PUB-2015-026, <https://cds.cern.ch/record/2037717>, 2015.
- [45] ATLAS Collaboration, ATLAS Pythia 8 tunes to 7 TeV data, ATL-PHYS-PUB-2014-021, <https://cds.cern.ch/record/1966419>, 2014.
- [46] R.D. Ball, et al., Parton distributions with LHC data, *Nucl. Phys. B* 867 (2013) 244, arXiv:1207.1303 [hep-ph].
- [47] CMS Collaboration, Measurement of prompt and nonprompt charmonium suppression in PbPb collisions at 5.02 TeV, *Eur. Phys. J. C* 78 (2018) 509, arXiv:1712.08959 [hep-ex].
- [48] CMS Collaboration, Prompt and non-prompt J/ψ production in pp collisions at $\sqrt{s} = 7$ TeV, *Eur. Phys. J. C* 71 (2011) 1575, arXiv:1011.4193 [hep-ex].
- [49] B. Alver, G. Roland, Collision-geometry fluctuations and triangular flow in heavy-ion collisions, *Phys. Rev. C* 81 (2010) 054905, arXiv:1003.0194 [nucl-th], Erratum, *Phys. Rev. C* 82 (2010) 039903.
- [50] W. Zhao, H. Xu, H. Song, Collective flow in 2.76 and 5.02 A TeV Pb+Pb collisions, *Eur. Phys. J. C* 77 (2017) 645, arXiv:1703.10792 [nucl-th].
- [51] R. Baier, Y.L. Dokshitzer, S. Peigne, D. Schiff, Induced gluon radiation in a QCD medium, *Phys. Lett. B* 345 (1995) 277, arXiv:hep-ph/9411409 [hep-ph].
- [52] C.A.G. Prado, et al., Event-by-event correlations between soft hadrons and D^0 mesons in 5.02 TeV PbPb collisions at the CERN large hadron collider, *Phys. Rev. C* 96 (2017) 064903, arXiv:1611.02965 [nucl-th].
- [53] J.D. Bjorken, Highly relativistic nucleus-nucleus collisions: the central rapidity region, *Phys. Rev. D* 27 (1983) 140.
- [54] J.S. Moreland, J.E. Bernhard, S.A. Bass, Alternative ansatz to wounded nucleon and binary collision scaling in high-energy nuclear collisions, *Phys. Rev. C* 92 (2015) 011901, arXiv:1412.4708 [nucl-th].
- [55] ATLAS Collaboration, Measurement of the azimuthal anisotropy for charged particle production in $\sqrt{s_{NN}} = 2.76$ TeV lead-lead collisions with the ATLAS detector, *Phys. Rev. C* 86 (2012) 014907, arXiv:1203.3087 [hep-ex].
- [56] ATLAS Collaboration, ATLAS computing acknowledgements, ATL-SOFT-PUB-2020-001, <https://cds.cern.ch/record/2717821>.

The ATLAS Collaboration

G. Aad¹⁰², B. Abbott¹²⁸, D.C. Abbott¹⁰³, A. Abed Abud³⁶, K. Abeling⁵³, D.K. Abhayasinghe⁹⁴, S.H. Abidi¹⁶⁶, O.S. AbouZeid⁴⁰, N.L. Abraham¹⁵⁵, H. Abramowicz¹⁶⁰, H. Abreu¹⁵⁹, Y. Abulaiti⁶, B.S. Acharya^{67a,67b,n}, B. Achkar⁵³, S. Adachi¹⁶², L. Adam¹⁰⁰, C. Adam Bourdarios⁵, L. Adamczyk^{84a}, L. Adamek¹⁶⁶, J. Adelman¹²¹, M. Adersberger¹¹⁴, A. Adiguzel^{12c}, S. Adorni⁵⁴, T. Adye¹⁴³, A.A. Affolder¹⁴⁵, Y. Afik¹⁵⁹, C. Agapopoulou⁶⁵, M.N. Agaras³⁸, A. Aggarwal¹¹⁹, C. Agheorghiesei^{27c}, J.A. Aguilar-Saavedra^{139f,139a,ae}, F. Ahmadov⁸⁰, W.S. Ahmed¹⁰⁴, X. Ai¹⁸, G. Aielli^{74a,74b}, S. Akatsuka⁸⁶, T.P.A. Åkesson⁹⁷, E. Akilli⁵⁴, A.V. Akimov¹¹¹, K. Al Khoury⁶⁵, G.L. Alberghi^{23b,23a}, J. Albert¹⁷⁵, M.J. Alconada Verzini¹⁶⁰, S. Alderweireldt³⁶, M. Aleksa³⁶, I.N. Aleksandrov⁸⁰, C. Alexa^{27b}, T. Alexopoulos¹⁰, A. Alfonsi¹²⁰, F. Alfonsi^{23b,23a}, M. Alhroob¹²⁸, B. Ali¹⁴¹, M. Aliev¹⁶⁵, G. Alimonti^{69a}, C. Allaire⁶⁵, B.M.M. Allbrooke¹⁵⁵, B.W. Allen¹³¹, P.P. Allport²¹, A. Aloisio^{70a,70b}, F. Alonso⁸⁹, C. Alpigiani¹⁴⁷, A.A. Alshehri⁵⁷, E. Alunno Camelia^{74a,74b}, M. Alvarez Estevez⁹⁹, M.G. Alviggi^{70a,70b}, Y. Amaral Coutinho^{81b}, A. Ambler¹⁰⁴, L. Ambroz¹³⁴, C. Amelung²⁶, D. Amidei¹⁰⁶, S.P. Amor Dos Santos^{139a}, S. Amoroso⁴⁶, C.S. Amrouche⁵⁴, F. An⁷⁹, C. Anastopoulos¹⁴⁸, N. Andari¹⁴⁴, T. Andeen¹¹, C.F. Anders^{61b}, J.K. Anders²⁰, S.Y. Andrean^{45a,45b}, A. Andreazza^{69a,69b}, V. Andrei^{61a}, C.R. Anelli¹⁷⁵, S. Angelidakis³⁸, A. Angerami³⁹, A.V. Anisenkov^{122b,122a}, A. Annovi^{72a}, C. Antel⁵⁴, M.T. Anthony¹⁴⁸, E. Antipov¹²⁹, M. Antonelli⁵¹, D.J.A. Antrim¹⁷⁰, F. Anulli^{73a}, M. Aoki⁸², J.A. Aparisi Pozo¹⁷³, M.A. Aparo¹⁵⁵, L. Aperio Bella^{15a}, J.P. Araque^{139a}, V. Araujo Ferraz^{81b}, R. Araujo Pereira^{81b}, C. Arcangeletti⁵¹, A.T.H. Arce⁴⁹, F.A. Arduh⁸⁹, J-F. Arguin¹¹⁰, S. Argyropoulos⁵², J.-H. Arling⁴⁶, A.J. Armbruster³⁶, A. Armstrong¹⁷⁰, O. Arnaez¹⁶⁶, H. Arnold¹²⁰, Z.P. Arrubarrena Tame¹¹⁴, G. Artoni¹³⁴, S. Artz¹⁰⁰, S. Asai¹⁶², T. Asawatavonvanich¹⁶⁴, N. Asbah⁵⁹, E.M. Asimakopoulou¹⁷¹, L. Asquith¹⁵⁵, J. Assahsah^{35d}, K. Assamagan²⁹, R. Astalos^{28a}, R.J. Atkin^{33a}, M. Atkinson¹⁷², N.B. Atlay¹⁹, H. Atmani⁶⁵, K. Augsten¹⁴¹, G. Avolio³⁶, M.K. Ayoub^{15a}, G. Azuelos^{110,an}, H. Bachacou¹⁴⁴, K. Bachas¹⁶¹, M. Backes¹³⁴, F. Backman^{45a,45b}, P. Bagnaia^{73a,73b}, M. Bahmani⁸⁵, H. Bahrasemani¹⁵¹, A.J. Bailey¹⁷³, V.R. Bailey¹⁷², J.T. Baines¹⁴³, C. Bakalis¹⁰, O.K. Baker¹⁸²,

P.J. Bakker¹²⁰, D. Bakshi Gupta⁸, S. Balaji¹⁵⁶, E.M. Baldin^{122b,122a}, P. Balek¹⁷⁹, F. Balli¹⁴⁴, W.K. Balunas¹³⁴, J. Balz¹⁰⁰, E. Banas⁸⁵, M. Bandieramonte¹³⁸, A. Bandyopadhyay²⁴, Sw. Banerjee^{180,i}, L. Barak¹⁶⁰, W.M. Barbe³⁸, E.L. Barberio¹⁰⁵, D. Barberis^{55b,55a}, M. Barbero¹⁰², G. Barbour⁹⁵, T. Barillari¹¹⁵, M-S. Barisits³⁶, J. Barkeloo¹³¹, T. Barklow¹⁵², R. Barnea¹⁵⁹, B.M. Barnett¹⁴³, R.M. Barnett¹⁸, Z. Barnovska-Blenessy^{60a}, A. Baroncelli^{60a}, G. Barone²⁹, A.J. Barr¹³⁴, L. Barranco Navarro^{45a,45b}, F. Barreiro⁹⁹, J. Barreiro Guimarães da Costa^{15a}, S. Barsov¹³⁷, F. Bartels^{61a}, R. Bartoldus¹⁵², G. Bartolini¹⁰², A.E. Barton⁹⁰, P. Bartos^{28a}, A. Basalae⁴⁶, A. Basan¹⁰⁰, A. Bassalat^{65,aj}, M.J. Basso¹⁶⁶, R.L. Bates⁵⁷, S. Batlamous^{35e}, J.R. Batley³², B. Batool¹⁵⁰, M. Battaglia¹⁴⁵, M. Bauce^{73a,73b}, F. Bauer¹⁴⁴, K.T. Bauer¹⁷⁰, H.S. Bawa³¹, J.B. Beacham⁴⁹, T. Beau¹³⁵, P.H. Beauchemin¹⁶⁹, F. Becherer⁵², P. Bechtel²⁴, H.C. Beck⁵³, H.P. Beck^{20,q}, K. Becker¹⁷⁷, C. Becot⁴⁶, A. Beddall^{12d}, A.J. Beddall^{12a}, V.A. Bednyakov⁸⁰, M. Bedognetti¹²⁰, C.P. Bee¹⁵⁴, T.A. Beermann¹⁸¹, M. Begalli^{81b}, M. Begel²⁹, A. Behera¹⁵⁴, J.K. Behr⁴⁶, F. Beisiegel²⁴, A.S. Bell⁹⁵, G. Bella¹⁶⁰, L. Bellagamba^{23b}, A. Bellerive³⁴, P. Bellos⁹, K. Beloborodov^{122b,122a}, K. Belotskiy¹¹², N.L. Belyaev¹¹², D. Benchekroun^{35a}, N. Benekos¹⁰, Y. Benhammou¹⁶⁰, D.P. Benjamin⁶, M. Benoit⁵⁴, J.R. Bensinger²⁶, S. Bentvelsen¹²⁰, L. Beresford¹³⁴, M. Beretta⁵¹, D. Berge¹⁹, E. Bergeaas Kuutmann¹⁷¹, N. Berger⁵, B. Bergmann¹⁴¹, L.J. Bergsten²⁶, J. Beringer¹⁸, S. Berlendis⁷, G. Bernardi¹³⁵, C. Bernius¹⁵², F.U. Bernlochner²⁴, T. Berry⁹⁴, P. Berta¹⁰⁰, C. Bertella^{15a}, I.A. Bertram⁹⁰, O. Bessidskaia Bylund¹⁸¹, N. Besson¹⁴⁴, A. Bethani¹⁰¹, S. Bethke¹¹⁵, A. Betti⁴², A.J. Bevan⁹³, J. Beyer¹¹⁵, D.S. Bhattacharya¹⁷⁶, P. Bhattarai²⁶, R. Bi¹³⁸, R.M. Bianchi¹³⁸, O. Biebel¹¹⁴, D. Biedermann¹⁹, R. Bielski³⁶, K. Bierwagen¹⁰⁰, N.V. Biesuz^{72a,72b}, M. Biglietti^{75a}, T.R.V. Billoud¹¹⁰, M. Bindi⁵³, A. Bingul^{12d}, C. Bini^{73a,73b}, S. Biondi^{23b,23a}, M. Birman¹⁷⁹, T. Bisanz⁵³, J.P. Biswal³, D. Biswas^{180,i}, A. Bitadze¹⁰¹, C. Bittrich⁴⁸, K. Bjørke¹³³, T. Blazek^{28a}, I. Bloch⁴⁶, C. Blocker²⁶, A. Blue⁵⁷, U. Blumenschein⁹³, G.J. Bobbink¹²⁰, V.S. Bobrovnikov^{122b,122a}, S.S. Bocchetta⁹⁷, A. Bocci⁴⁹, D. Boerner⁴⁶, D. Bogavac¹⁴, A.G. Bogdanchikov^{122b,122a}, C. Böhm^{45a}, V. Boisvert⁹⁴, P. Boka^{53,171}, T. Bold^{84a}, A.E. Bolz^{61b}, M. Bomben¹³⁵, M. Bona⁹³, J.S. Bonilla¹³¹, M. Boonekamp¹⁴⁴, C.D. Booth⁹⁴, H.M. Borecka-Bielska⁹¹, L.S. Borgna⁹⁵, A. Borisov¹²³, G. Borissov⁹⁰, J. Bortfeldt³⁶, D. Bortoletto¹³⁴, D. Boscherini^{23b}, M. Bosman¹⁴, J.D. Bossio Sola¹⁰⁴, K. Bouaouda^{35a}, J. Boudreau¹³⁸, E.V. Bouhova-Thacker⁹⁰, D. Boumediene³⁸, S.K. Boutle⁵⁷, A. Boveia¹²⁷, J. Boyd³⁶, D. Boye^{33c,ak}, I.R. Boyko⁸⁰, A.J. Bozson⁹⁴, J. Bracinik²¹, N. Brahimi¹⁰², G. Brandt¹⁸¹, O. Brandt³², F. Braren⁴⁶, B. Brau¹⁰³, J.E. Brau¹³¹, W.D. Breaden Madden⁵⁷, K. Brendlinger⁴⁶, L. Brenner⁴⁶, R. Brenner¹⁷¹, S. Bressler¹⁷⁹, B. Brickwedde¹⁰⁰, D.L. Briglin²¹, D. Britton⁵⁷, D. Britzger¹¹⁵, I. Brock²⁴, R. Brock¹⁰⁷, G. Brooijmans³⁹, W.K. Brooks^{146d}, E. Brost²⁹, J.H. Broughton²¹, P.A. Bruckman de Renstrom⁸⁵, D. Bruncko^{28b}, A. Bruni^{23b}, G. Bruni^{23b}, L.S. Bruni¹²⁰, S. Bruno^{74a,74b}, M. Bruschi^{23b}, N. Bruscino^{73a,73b}, L. Bryngemark⁹⁷, T. Buanes¹⁷, Q. Buat³⁶, P. Buchholz¹⁵⁰, A.G. Buckley⁵⁷, I.A. Budagov⁸⁰, M.K. Bugge¹³³, F. Bühner⁵², O. Bulekov¹¹², T.J. Burch¹²¹, S. Burdin⁹¹, C.D. Burgard¹²⁰, A.M. Burger¹²⁹, B. Burghgrave⁸, J.T.P. Burr⁴⁶, C.D. Burton¹¹, J.C. Burzynski¹⁰³, V. Büscher¹⁰⁰, E. Buschmann⁵³, P.J. Bussey⁵⁷, J.M. Butler²⁵, C.M. Buttar⁵⁷, J.M. Butterworth⁹⁵, P. Butti³⁶, W. Buttinger³⁶, C.J. Buxo Vazquez¹⁰⁷, A. Buzatu¹⁵⁷, A.R. Buzykaev^{122b,122a}, G. Cabras^{23b,23a}, S. Cabrera Urbán¹⁷³, D. Caforio⁵⁶, H. Cai¹⁷², V.M.M. Cairo¹⁵², O. Cakir^{4a}, N. Calace³⁶, P. Calafiura¹⁸, G. Calderini¹³⁵, P. Calfayan⁶⁶, G. Callea⁵⁷, L.P. Caloba^{81b}, A. Caltabiano^{74a,74b}, S. Calvente Lopez⁹⁹, D. Calvet³⁸, S. Calvet³⁸, T.P. Calvet¹⁵⁴, M. Calvetti^{72a,72b}, R. Camacho Toro¹³⁵, S. Camarda³⁶, D. Camarero Munoz⁹⁹, P. Camarri^{74a,74b}, D. Cameron¹³³, C. Camincher³⁶, S. Campana³⁶, M. Campanelli⁹⁵, A. Camplani⁴⁰, A. Campoverde¹⁵⁰, V. Canale^{70a,70b}, A. Canesse¹⁰⁴, M. Cano Bret^{60c}, J. Cantero¹²⁹, T. Cao¹⁶⁰, Y. Cao¹⁷², M.D.M. Capeans Garrido³⁶, M. Capua^{41b,41a}, R. Cardarelli^{74a}, F. Cardillo¹⁴⁸, G. Carducci^{41b,41a}, I. Carli¹⁴², T. Carli³⁶, G. Carlino^{70a}, B.T. Carlson¹³⁸, E.M. Carlson^{175,167a}, L. Carminati^{69a,69b}, R.M.D. Carney¹⁵², S. Caron¹¹⁹, E. Carquin^{146d}, S. Carrá⁴⁶, J.W.S. Carter¹⁶⁶, M.P. Casado^{14,e}, A.F. Casha¹⁶⁶, F.L. Castillo¹⁷³, L. Castillo Garcia¹⁴, V. Castillo Gimenez¹⁷³, N.F. Castro^{139a,139e}, A. Catinaccio³⁶, J.R. Catmore¹³³, A. Cattai³⁶, V. Cavaliere²⁹, E. Cavallaro¹⁴, M. Cavalli-Sforza¹⁴, V. Cavasinni^{72a,72b}, E. Celebi^{12b}, L. Cerda Alberich¹⁷³, K. Cerny¹³⁰, A.S. Cerqueira^{81a}, A. Cerri¹⁵⁵, L. Cerrito^{74a,74b}, F. Cerutti¹⁸, A. Cervelli^{23b,23a}, S.A. Cetin^{12b}, Z. Chadi^{35a}, D. Chakraborty¹²¹, J. Chan¹⁸⁰, W.S. Chan¹²⁰, W.Y. Chan⁹¹, J.D. Chapman³², B. Chargeishvili^{158b}, D.G. Charlton²¹, T.P. Charman⁹³, C.C. Chau³⁴, S. Che¹²⁷, S. Chekanov⁶, S.V. Chekulaev^{167a}, G.A. Chelkov^{80,ah}, B. Chen⁷⁹, C. Chen^{60a}, C.H. Chen⁷⁹, H. Chen²⁹, J. Chen^{60a}, J. Chen³⁹, J. Chen²⁶, S. Chen¹³⁶, S.J. Chen^{15c}, X. Chen^{15b}, Y-H. Chen⁴⁶, H.C. Cheng^{63a}, H.J. Cheng^{15a}, A. Cheplakov⁸⁰, E. Cheremushkina¹²³,

R. Cherkaoui El Moursli ^{35e}, E. Cheu ⁷, K. Cheung ⁶⁴, T.J.A. Chevaléras ¹⁴⁴, L. Chevalier ¹⁴⁴, V. Chiarella ⁵¹, G. Chiarelli ^{72a}, G. Chiodini ^{68a}, A.S. Chisholm ²¹, A. Chitan ^{27b}, I. Chiu ¹⁶², Y.H. Chiu ¹⁷⁵, M.V. Chizhov ⁸⁰, K. Choi ¹¹, A.R. Chomont ^{73a,73b}, S. Chouridou ¹⁶¹, Y.S. Chow ¹²⁰, M.C. Chu ^{63a}, X. Chu ^{15a,15d}, J. Chudoba ¹⁴⁰, J.J. Chwastowski ⁸⁵, L. Chytka ¹³⁰, D. Cieri ¹¹⁵, K.M. Ciesla ⁸⁵, D. Cinca ⁴⁷, V. Cindro ⁹², I.A. Cioară ^{27b}, A. Ciochio ¹⁸, F. Ciotto ^{70a,70b}, Z.H. Citron ^{179,j}, M. Citterio ^{69a}, D.A. Ciubotaru ^{27b}, B.M. Ciungu ¹⁶⁶, A. Clark ⁵⁴, M.R. Clark ³⁹, P.J. Clark ⁵⁰, C. Clement ^{45a,45b}, Y. Coadou ¹⁰², M. Cobal ^{67a,67c}, A. Coccaro ^{55b}, J. Cochran ⁷⁹, R. Coelho Lopes De Sa ¹⁰³, H. Cohen ¹⁶⁰, A.E.C. Coimbra ³⁶, B. Cole ³⁹, A.P. Colijn ¹²⁰, J. Collot ⁵⁸, P. Conde Muiño ^{139a,139h}, S.H. Connell ^{33c}, I.A. Connelly ⁵⁷, S. Constantinescu ^{27b}, F. Conventi ^{70a,ao}, A.M. Cooper-Sarkar ¹³⁴, F. Cormier ¹⁷⁴, K.J.R. Cormier ¹⁶⁶, L.D. Corpe ⁹⁵, M. Corradi ^{73a,73b}, E.E. Corrigan ⁹⁷, F. Corriveau ^{104,ac}, M.J. Costa ¹⁷³, F. Costanza ⁵, D. Costanzo ¹⁴⁸, G. Cowan ⁹⁴, J.W. Cowley ³², J. Crane ¹⁰¹, K. Cranmer ¹²⁵, S.J. Crawley ⁵⁷, R.A. Creager ¹³⁶, S. Crépe-Renaudin ⁵⁸, F. Crescioli ¹³⁵, M. Cristinziani ²⁴, V. Croft ¹⁶⁹, G. Crosetti ^{41b,41a}, A. Cueto ⁵, T. Cuhadar Donszelmann ¹⁷⁰, A.R. Cukierman ¹⁵², W.R. Cunningham ⁵⁷, S. Czekierda ⁸⁵, P. Czodrowski ³⁶, M.M. Czurylo ^{61b}, M.J. Da Cunha Sargedas De Sousa ^{60b}, J.V. Da Fonseca Pinto ^{81b}, C. Da Via ¹⁰¹, W. Dabrowski ^{84a}, F. Dachs ³⁶, T. Dado ^{28a}, S. Dahbi ^{33e}, T. Dai ¹⁰⁶, C. Dallapiccola ¹⁰³, M. Dam ⁴⁰, G. D'amen ²⁹, V. D'Amico ^{75a,75b}, J. Damp ¹⁰⁰, J.R. Dandoy ¹³⁶, M.F. Daneri ³⁰, N.S. Dann ¹⁰¹, M. Danninger ¹⁵¹, V. Dao ³⁶, G. Darbo ^{55b}, O. Dartsis ⁵, A. Dattagupta ¹³¹, T. Daubney ⁴⁶, S. D'Auria ^{69a,69b}, C. David ^{167b}, T. Davidek ¹⁴², D.R. Davis ⁴⁹, I. Dawson ¹⁴⁸, K. De ⁸, R. De Asmundis ^{70a}, M. De Beurs ¹²⁰, S. De Castro ^{23b,23a}, S. De Cecco ^{73a,73b}, N. De Groot ¹¹⁹, P. de Jong ¹²⁰, H. De la Torre ¹⁰⁷, A. De Maria ^{15c}, D. De Pedis ^{73a}, A. De Salvo ^{73a}, U. De Sanctis ^{74a,74b}, M. De Santis ^{74a,74b}, A. De Santo ¹⁵⁵, K. De Vasconcelos Corga ¹⁰², J.B. De Vivie De Regie ⁶⁵, C. Debenedetti ¹⁴⁵, D.V. Dedovich ⁸⁰, A.M. Deiana ⁴², J. Del Peso ⁹⁹, Y. Delabat Diaz ⁴⁶, D. Delgove ⁶⁵, F. Deliot ^{144,p}, C.M. Delitzsch ⁷, M. Della Pietra ^{70a,70b}, D. Della Volpe ⁵⁴, A. Dell'Acqua ³⁶, L. Dell'Asta ^{74a,74b}, M. Delmastro ⁵, C. Delporte ⁶⁵, P.A. Delsart ⁵⁸, D.A. DeMarco ¹⁶⁶, S. Demers ¹⁸², M. Demichev ⁸⁰, G. Demontigny ¹¹⁰, S.P. Denisov ¹²³, L. D'Eramo ¹³⁵, D. Derendarz ⁸⁵, J.E. Derkaoui ^{35d}, F. Derue ¹³⁵, P. Dervan ⁹¹, K. Desch ²⁴, C. Deterre ⁴⁶, K. Dette ¹⁶⁶, C. Deutsch ²⁴, M.R. Devesa ³⁰, P.O. Deviveiros ³⁶, F.A. Di Bello ^{73a,73b}, A. Di Ciaccio ^{74a,74b}, L. Di Ciaccio ⁵, W.K. Di Clemente ¹³⁶, C. Di Donato ^{70a,70b}, A. Di Girolamo ³⁶, G. Di Gregorio ^{72a,72b}, B. Di Micco ^{75a,75b}, R. Di Nardo ^{75a,75b}, K.F. Di Petrillo ⁵⁹, R. Di Sipio ¹⁶⁶, C. Diaconu ¹⁰², F.A. Dias ⁴⁰, T. Dias Do Vale ^{139a}, M.A. Diaz ^{146a}, J. Dickinson ¹⁸, E.B. Diehl ¹⁰⁶, J. Dietrich ¹⁹, S. Díez Cornell ⁴⁶, A. Dimitrievska ¹⁸, W. Ding ^{15b}, J. Dingfelder ²⁴, F. Dittus ³⁶, F. Djama ¹⁰², T. Djobava ^{158b}, J.I. Djuvsland ¹⁷, M.A.B. Do Vale ^{81c}, M. Dobre ^{27b}, D. Dodsworth ²⁶, C. Doglioni ⁹⁷, J. Dolejsi ¹⁴², Z. Dolezal ¹⁴², M. Donadelli ^{81d}, B. Dong ^{60c}, J. Donini ³⁸, A. D'onofrio ^{15c}, M. D'Onofrio ⁹¹, J. Dopke ¹⁴³, A. Doria ^{70a}, M.T. Dova ⁸⁹, A.T. Doyle ⁵⁷, E. Drechsler ¹⁵¹, E. Dreyer ¹⁵¹, T. Dreyer ⁵³, A.S. Drobac ¹⁶⁹, D. Du ^{60b}, Y. Duan ^{60b}, F. Dubinin ¹¹¹, M. Dubovsky ^{28a}, A. Dubreuil ⁵⁴, E. Duchovni ¹⁷⁹, G. Duckeck ¹¹⁴, A. Ducourthial ¹³⁵, O.A. Ducu ¹¹⁰, D. Duda ¹¹⁵, A. Dudarev ³⁶, A.C. Dudder ¹⁰⁰, E.M. Duffield ¹⁸, L. Duflo ⁶⁵, M. Dührssen ³⁶, C. Dülsen ¹⁸¹, M. Dumancic ¹⁷⁹, A.E. Dumitriu ^{27b}, A.K. Duncan ⁵⁷, M. Dunford ^{61a}, A. Duperrin ¹⁰², H. Duran Yildiz ^{4a}, M. Düren ⁵⁶, A. Durglishvili ^{158b}, D. Duschinger ⁴⁸, B. Dutta ⁴⁶, D. Duvnjak ¹, G.I. Dyckes ¹³⁶, M. Dyndal ³⁶, S. Dysch ¹⁰¹, B.S. Dziedzic ⁸⁵, K.M. Ecker ¹¹⁵, M.G. Eggleston ⁴⁹, T. Eifert ⁸, G. Eigen ¹⁷, K. Einsweiler ¹⁸, T. Ekelof ¹⁷¹, H. El Jarrari ^{35e}, R. El Kosseifi ¹⁰², V. Ellajosyula ¹⁷¹, M. Ellert ¹⁷¹, F. Ellinghaus ¹⁸¹, A.A. Elliot ⁹³, N. Ellis ³⁶, J. Elmsheuser ²⁹, M. Elsing ³⁶, D. Emeliyanov ¹⁴³, A. Emerman ³⁹, Y. Enari ¹⁶², M.B. Epland ⁴⁹, J. Erdmann ⁴⁷, A. Ereditato ²⁰, P.A. Erland ⁸⁵, M. Errenst ³⁶, M. Escalier ⁶⁵, C. Escobar ¹⁷³, O. Estrada Pastor ¹⁷³, E. Etzion ¹⁶⁰, H. Evans ⁶⁶, M.O. Evans ¹⁵⁵, A. Ezhilov ¹³⁷, F. Fabbri ⁵⁷, L. Fabbri ^{23b,23a}, V. Fabiani ¹¹⁹, G. Facini ¹⁷⁷, R.M. Faisca Rodrigues Pereira ^{139a}, R.M. Fakhrutdinov ¹²³, S. Falciano ^{73a}, P.J. Falke ⁵, S. Falke ⁵, J. Faltova ¹⁴², Y. Fang ^{15a}, Y. Fang ^{15a}, G. Fanourakis ⁴⁴, M. Fanti ^{69a,69b}, M. Faraj ^{67a,67c,r}, A. Farbin ⁸, A. Farilla ^{75a}, E.M. Farina ^{71a,71b}, T. Farooque ¹⁰⁷, S.M. Farrington ⁵⁰, P. Farthouat ³⁶, F. Fassi ^{35e}, P. Fassnacht ³⁶, D. Fassouliotis ⁹, M. Fauci Giannelli ⁵⁰, W.J. Fawcett ³², L. Fayard ⁶⁵, O.L. Fedin ^{137,o}, W. Fedorko ¹⁷⁴, A. Fehr ²⁰, M. Feickert ¹⁷², L. Feligioni ¹⁰², A. Fell ¹⁴⁸, C. Feng ^{60b}, M. Feng ⁴⁹, M.J. Fenton ¹⁷⁰, A.B. Fenyuk ¹²³, S.W. Ferguson ⁴³, J. Ferrando ⁴⁶, A. Ferrante ¹⁷², A. Ferrari ¹⁷¹, P. Ferrari ¹²⁰, R. Ferrari ^{71a}, D.E. Ferreira de Lima ^{61b}, A. Ferrer ¹⁷³, D. Ferrere ⁵⁴, C. Ferretti ¹⁰⁶, F. Fiedler ¹⁰⁰, A. Filipčič ⁹², F. Filthaut ¹¹⁹, K.D. Finelli ²⁵, M.C.N. Fiolhais ^{139a,139c,a}, L. Fiorini ¹⁷³, F. Fischer ¹¹⁴, W.C. Fisher ¹⁰⁷, I. Fleck ¹⁵⁰, P. Fleischmann ¹⁰⁶, T. Flick ¹⁸¹, B.M. Flierl ¹¹⁴, L. Flores ¹³⁶, L.R. Flores Castillo ^{63a}, F.M. Follega ^{76a,76b}, N. Fomin ¹⁷, J.H. Foo ¹⁶⁶, G.T. Forcolin ^{76a,76b}, A. Formica ¹⁴⁴,

F.A. Förster¹⁴, A.C. Forti¹⁰¹, A.G. Foster²¹, M.G. Foti¹³⁴, D. Fournier⁶⁵, H. Fox⁹⁰, P. Francavilla^{72a,72b}, S. Francescato^{73a,73b}, M. Franchini^{23b,23a}, S. Franchino^{61a}, D. Francis³⁶, L. Franconi²⁰, M. Franklin⁵⁹, A.N. Fray⁹³, P.M. Freeman²¹, B. Freund¹¹⁰, W.S. Freund^{81b}, E.M. Freundlich⁴⁷, D.C. Frizzell¹²⁸, D. Froidevaux³⁶, J.A. Frost¹³⁴, C. Fukunaga¹⁶³, E. Fullana Torregrosa¹⁷³, T. Fusayasu¹¹⁶, J. Fuster¹⁷³, A. Gabrielli^{23b,23a}, A. Gabrielli¹⁸, S. Gadatsch⁵⁴, P. Gadow¹¹⁵, G. Gagliardi^{55b,55a}, L.G. Gagnon¹¹⁰, B. Galhardo^{139a}, G.E. Gallardo¹³⁴, E.J. Gallas¹³⁴, B.J. Gallop¹⁴³, G. Galster⁴⁰, R. Gamboa Goni⁹³, K.K. Gan¹²⁷, S. Ganguly¹⁷⁹, J. Gao^{60a}, Y. Gao⁵⁰, Y.S. Gao^{31,l}, C. García¹⁷³, J.E. García Navarro¹⁷³, J.A. García Pascual^{15a}, C. Garcia-Argos⁵², M. Garcia-Sciveres¹⁸, R.W. Gardner³⁷, N. Garelli¹⁵², S. Gargiulo⁵², C.A. Garner¹⁶⁶, V. Garonne¹³³, S.J. Gasiorowski¹⁴⁷, P. Gaspar^{81b}, A. Gaudiello^{55b,55a}, G. Gaudio^{71a}, I.L. Gavrilenko¹¹¹, A. Gavrilyuk¹²⁴, C. Gay¹⁷⁴, G. Gaycken⁴⁶, E.N. Gazis¹⁰, A.A. Geanta^{27b}, C.M. Gee¹⁴⁵, C.N.P. Gee¹⁴³, J. Geisen⁹⁷, M. Geisen¹⁰⁰, C. Gemme^{55b}, M.H. Genest⁵⁸, C. Geng¹⁰⁶, S. Gentile^{73a,73b}, S. George⁹⁴, T. Geralis⁴⁴, L.O. Gerlach⁵³, P. Gessinger-Befurt¹⁰⁰, G. Gessner⁴⁷, S. Ghasemi¹⁵⁰, M. Ghasemi Bostanabad¹⁷⁵, M. Ghneimat¹⁵⁰, A. Ghosh⁶⁵, A. Ghosh⁷⁸, B. Giacobbe^{23b}, S. Giagu^{73a,73b}, N. Giangiacomi^{23b,23a}, P. Giannetti^{72a}, A. Giannini^{70a,70b}, G. Giannini¹⁴, S.M. Gibson⁹⁴, M. Gignac¹⁴⁵, D. Gillberg³⁴, G. Gilles¹⁸¹, D.M. Gingrich^{3,an}, M.P. Giordani^{67a,67c}, P.F. Giraud¹⁴⁴, G. Giugliarelli^{67a,67c}, D. Giugni^{69a}, F. Giuli^{74a,74b}, S. Gkaitatzis¹⁶¹, I. Gkialas^{9,g}, E.L. Gkougkousis¹⁴, P. Gkoutoumis¹⁰, L.K. Gladilin¹¹³, C. Glasman⁹⁹, J. Glatzer¹⁴, P.C.F. Glaysheer⁴⁶, A. Glazov⁴⁶, G.R. Gledhill¹³¹, I. Gnesi^{41b}, M. Goblirsch-Kolb²⁶, D. Godin¹¹⁰, S. Goldfarb¹⁰⁵, T. Golling⁵⁴, D. Golubkov¹²³, A. Gomes^{139a,139b}, R. Goncalves Gama⁵³, R. Gonçalves^{139a}, G. Gonella¹³¹, L. Gonella²¹, A. Gongadze⁸⁰, F. Gonnella²¹, J.L. Gonski³⁹, S. González de la Hoz¹⁷³, S. Gonzalez Fernandez¹⁴, C. Gonzalez Renteria¹⁸, S. Gonzalez-Sevilla⁵⁴, G.R. Gonzalvo Rodriguez¹⁷³, L. Goossens³⁶, N.A. Gorasia²¹, P.A. Gorbounov¹²⁴, H.A. Gordon²⁹, B. Gorini³⁶, E. Gorini^{68a,68b}, A. Gorišek⁹², A.T. Goshaw⁴⁹, M.I. Gostkin⁸⁰, C.A. Gottardo¹¹⁹, M. Gouighri^{35b}, A.G. Goussiou¹⁴⁷, N. Govender^{33c}, C. Goy⁵, E. Gozani¹⁵⁹, I. Grabowska-Bold^{84a}, E.C. Graham⁹¹, J. Gramling¹⁷⁰, E. Gramstad¹³³, S. Grancagnolo¹⁹, M. Grandi¹⁵⁵, V. Gratchev¹³⁷, P.M. Gravila^{27f}, F.G. Gravili^{68a,68b}, C. Gray⁵⁷, H.M. Gray¹⁸, C. Grefe²⁴, K. Gregersen⁹⁷, I.M. Gregor⁴⁶, P. Grenier¹⁵², K. Grevtsov⁴⁶, C. Grieco¹⁴, N.A. Grieser¹²⁸, A.A. Grillo¹⁴⁵, K. Grimm^{31,k}, S. Grinstein^{14,x}, J.-F. Grivaz⁶⁵, S. Groh¹⁰⁰, E. Gross¹⁷⁹, J. Grosse-Knetter⁵³, Z.J. Grout⁹⁵, C. Grud¹⁰⁶, A. Grummer¹¹⁸, L. Guan¹⁰⁶, W. Guan¹⁸⁰, C. Gubbels¹⁷⁴, J. Guenther³⁶, A. Guerguichon⁶⁵, J.G.R. Guerrero Rojas¹⁷³, F. Guescini¹¹⁵, D. Guest¹⁷⁰, R. Gugel⁵², T. Guillemain⁵, S. Guindon³⁶, U. Gul⁵⁷, J. Guo^{60c}, W. Guo¹⁰⁶, Y. Guo^{60a}, Z. Guo¹⁰², R. Gupta⁴⁶, S. Gurbuz^{12c}, G. Gustavino¹²⁸, M. Guth⁵², P. Gutierrez¹²⁸, C. Gutsche⁹⁵, C. Guyot¹⁴⁴, C. Gwenlan¹³⁴, C.B. Gwilliam⁹¹, A. Haas¹²⁵, C. Haber¹⁸, H.K. Hadavand⁸, A. Hadeef^{60a}, M. Haleem¹⁷⁶, J. Haley¹²⁹, G. Halladjian¹⁰⁷, G.D. Hallewell¹⁰², K. Hamacher¹⁸¹, P. Hamal¹³⁰, K. Hamano¹⁷⁵, H. Hamdaoui^{35e}, M. Hamer²⁴, G.N. Hamity⁵⁰, K. Han^{60a,w}, L. Han^{60a}, S. Han^{15a}, Y.F. Han¹⁶⁶, K. Hanagaki^{82,u}, M. Hance¹⁴⁵, D.M. Handl¹¹⁴, B. Haney¹³⁶, R. Hankache¹³⁵, E. Hansen⁹⁷, J.B. Hansen⁴⁰, J.D. Hansen⁴⁰, M.C. Hansen²⁴, P.H. Hansen⁴⁰, E.C. Hanson¹⁰¹, K. Hara¹⁶⁸, T. Harenberg¹⁸¹, S. Harkusha¹⁰⁸, P.F. Harrison¹⁷⁷, N.M. Hartman¹⁵², N.M. Hartmann¹¹⁴, Y. Hasegawa¹⁴⁹, A. Hasib⁵⁰, S. Hassani¹⁴⁴, S. Haug²⁰, R. Hauser¹⁰⁷, L.B. Havener³⁹, M. Havranek¹⁴¹, C.M. Hawkes²¹, R.J. Hawkins³⁶, D. Hayden¹⁰⁷, C. Hayes¹⁰⁶, R.L. Hayes¹⁷⁴, C.P. Hays¹³⁴, J.M. Hays⁹³, H.S. Hayward⁹¹, S.J. Haywood¹⁴³, F. He^{60a}, M.P. Heath⁵⁰, V. Hedberg⁹⁷, S. Heer²⁴, K.K. Heidegger⁵², W.D. Heidorn⁷⁹, J. Heilman³⁴, S. Heim⁴⁶, T. Heim¹⁸, B. Heinemann^{46,al}, J.J. Heinrich¹³¹, L. Heinrich³⁶, J. Hejbal¹⁴⁰, L. Helary^{61b}, A. Held¹²⁵, S. Hellesund¹³³, C.M. Helling¹⁴⁵, S. Hellman^{45a,45b}, C. Helsens³⁶, R.C.W. Henderson⁹⁰, Y. Heng¹⁸⁰, L. Henkelmann³², A.M. Henriques Correia³⁶, H. Herde²⁶, Y. Hernández Jiménez^{33e}, H. Herr¹⁰⁰, M.G. Herrmann¹¹⁴, T. Herrmann⁴⁸, G. Herten⁵², R. Hertenberger¹¹⁴, L. Hervas³⁶, T.C. Herwig¹³⁶, G.G. Hesketh⁹⁵, N.P. Hessey^{167a}, H. Hibi⁸³, A. Higashida¹⁶², S. Higashino⁸², E. Higón-Rodríguez¹⁷³, K. Hildebrand³⁷, J.C. Hill³², K.K. Hill²⁹, K.H. Hiller⁴⁶, S.J. Hillier²¹, M. Hils⁴⁸, I. Hinchliffe¹⁸, F. Hinterkeuser²⁴, M. Hirose¹³², S. Hirose⁵², D. Hirschbuehl¹⁸¹, B. Hiti⁹², O. Hladik¹⁴⁰, D.R. Hlaluku^{33e}, J. Hobbs¹⁵⁴, N. Hod¹⁷⁹, M.C. Hodgkinson¹⁴⁸, A. Hoecker³⁶, D. Hohn⁵², D. Hohov⁶⁵, T. Holm²⁴, T.R. Holmes³⁷, M. Holzbock¹¹⁴, L.B.A.H. Hommels³², S. Honda¹⁶⁸, T.M. Hong¹³⁸, J.C. Honig⁵², A. Hönle¹¹⁵, B.H. Hooberman¹⁷², W.H. Hopkins⁶, Y. Horii¹¹⁷, P. Horn⁴⁸, L.A. Horyn³⁷, S. Hou¹⁵⁷, A. Hoummada^{35a}, J. Howarth⁵⁷, J. Hoya⁸⁹, M. Hrabovsky¹³⁰, J. Hrdinka⁷⁷, I. Hristova¹⁹, J. Hrivnac⁶⁵, A. Hrynevich¹⁰⁹, T. Hryn'ova⁵, P.J. Hsu⁶⁴, S.-C. Hsu¹⁴⁷, Q. Hu²⁹, S. Hu^{60c}, Y.F. Hu^{15a,15d}, D.P. Huang⁹⁵, Y. Huang^{60a}, Y. Huang^{15a}, Z. Hubacek¹⁴¹, F. Hubaut¹⁰², M. Huebner²⁴, F. Huegging²⁴,

T.B. Huffman¹³⁴, M. Huhtinen³⁶, R.F.H. Hunter³⁴, P. Huo¹⁵⁴, N. Huseynov^{80,ad}, J. Huston¹⁰⁷, J. Huth⁵⁹, R. Hyneman¹⁰⁶, S. Hyrych^{28a}, G. Iacobucci⁵⁴, G. Iakovidis²⁹, I. Ibragimov¹⁵⁰, L. Iconomidou-Fayard⁶⁵, P. Iengo³⁶, R. Ignazzi⁴⁰, O. Igonkina^{120,z,*}, R. Iguchi¹⁶², T. Iizawa⁵⁴, Y. Ikegami⁸², M. Ikeno⁸², D. Iliadis¹⁶¹, N. Ilic^{119,166,ac}, F. Iltzsche⁴⁸, G. Introzzi^{71a,71b}, M. Iodice^{75a}, K. Iordanidou^{167a}, V. Ippolito^{73a,73b}, M.F. Isacson¹⁷¹, M. Ishino¹⁶², W. Islam¹²⁹, C. Issever^{19,46}, S. Istin¹⁵⁹, F. Ito¹⁶⁸, J.M. Iturbe Ponce^{63a}, R. Iuppa^{76a,76b}, A. Ivina¹⁷⁹, H. Iwasaki⁸², J.M. Izen⁴³, V. Izzo^{70a}, P. Jacka¹⁴⁰, P. Jackson¹, R.M. Jacobs²⁴, B.P. Jaeger¹⁵¹, V. Jain², G. Jäkel¹⁸¹, K.B. Jakobi¹⁰⁰, K. Jakobs⁵², T. Jakoubek¹⁴⁰, J. Jamieson⁵⁷, K.W. Janas^{84a}, R. Jansky⁵⁴, M. Janus⁵³, P.A. Janus^{84a}, G. Jarlskog⁹⁷, A.E. Jaspan⁹¹, N. Javadov^{80,ad}, T. Javůrek³⁶, M. Javurkova¹⁰³, F. Jeanneau¹⁴⁴, L. Jeanty¹³¹, J. Jejelava^{158a}, A. Jelinskas¹⁷⁷, P. Jenni^{52,b}, N. Jeong⁴⁶, S. Jézéquel⁵, H. Ji¹⁸⁰, J. Jia¹⁵⁴, H. Jiang⁷⁹, Y. Jiang^{60a}, Z. Jiang¹⁵², S. Jiggins⁵², F.A. Jimenez Morales³⁸, J. Jimenez Pena¹¹⁵, S. Jin^{15c}, A. Jinaru^{27b}, O. Jinnouchi¹⁶⁴, H. Jivan^{33e}, P. Johansson¹⁴⁸, K.A. Johns⁷, C.A. Johnson⁶⁶, R.W.L. Jones⁹⁰, S.D. Jones¹⁵⁵, S. Jones⁷, T.J. Jones⁹¹, J. Jongmanns^{61a}, P.M. Jorge^{139a}, J. Jovicevic³⁶, X. Ju¹⁸, J.J. Junggeburth¹¹⁵, A. Juste Rozas^{14,x}, A. Kaczmarska⁸⁵, M. Kado^{73a,73b}, H. Kagan¹²⁷, M. Kagan¹⁵², A. Kahn³⁹, C. Kahra¹⁰⁰, T. Kaji¹⁷⁸, E. Kajomovitz¹⁵⁹, C.W. Kalderon²⁹, A. Kaluza¹⁰⁰, A. Kamenshchikov¹²³, M. Kaneda¹⁶², N.J. Kang¹⁴⁵, S. Kang⁷⁹, Y. Kano¹¹⁷, J. Kanzaki⁸², L.S. Kaplan¹⁸⁰, D. Kar^{33e}, K. Karava¹³⁴, M.J. Kareem^{167b}, I. Karkanas¹⁶¹, S.N. Karpov⁸⁰, Z.M. Karpova⁸⁰, V. Kartvelishvili⁹⁰, A.N. Karyukhin¹²³, A. Kastanas^{45a,45b}, C. Kato^{60d,60c}, J. Katzy⁴⁶, K. Kawade¹⁴⁹, K. Kawagoe⁸⁸, T. Kawaguchi¹¹⁷, T. Kawamoto¹⁴⁴, G. Kawamura⁵³, E.F. Kay¹⁷⁵, V.F. Kazanin^{122b,122a}, R. Keeler¹⁷⁵, R. Kehoe⁴², J.S. Keller³⁴, E. Kellermann⁹⁷, D. Kelsey¹⁵⁵, J.J. Kempster²¹, J. Kendrick²¹, K.E. Kennedy³⁹, O. Kepka¹⁴⁰, S. Kersten¹⁸¹, B.P. Kerševan⁹², S. Ketabchi Haghighat¹⁶⁶, M. Khader¹⁷², F. Khalil-Zada¹³, M. Khandoga¹⁴⁴, A. Khanov¹²⁹, A.G. Kharlamov^{122b,122a}, T. Kharlamova^{122b,122a}, E.E. Khoda¹⁷⁴, A. Khodinov¹⁶⁵, T.J. Khoo⁵⁴, E. Khramov⁸⁰, J. Khubua^{158b}, S. Kido⁸³, M. Kiehn⁵⁴, C.R. Kilby⁹⁴, E. Kim¹⁶⁴, Y.K. Kim³⁷, N. Kimura⁹⁵, O.M. Kind¹⁹, B.T. King^{91,*}, D. Kirchmeier⁴⁸, J. Kirk¹⁴³, A.E. Kiryunin¹¹⁵, T. Kishimoto¹⁶², D.P. Kisliuk¹⁶⁶, V. Kitali⁴⁶, O. Kivernyk²⁴, T. Klapdor-Kleingrothaus⁵², M. Klassen^{61a}, C. Klein³⁴, M.H. Klein¹⁰⁶, M. Klein⁹¹, U. Klein⁹¹, K. Kleinknecht¹⁰⁰, P. Klimek¹²¹, A. Klimentov²⁹, T. Klingl²⁴, T. Klioutchnikova³⁶, F.F. Klitzner¹¹⁴, P. Kluit¹²⁰, S. Kluth¹¹⁵, E. Kneringer⁷⁷, E.B.F.G. Knoop¹⁰², A. Knue⁵², D. Kobayashi⁸⁸, T. Kobayashi¹⁶², M. Kobel⁴⁸, M. Kocian¹⁵², T. Kodama¹⁶², P. Kodys¹⁴², D.M. Koeck¹⁵⁵, P.T. Koenig²⁴, T. Koffas³⁴, N.M. Köhler³⁶, M. Kolb¹⁴⁴, I. Koletsou⁵, T. Komarek¹³⁰, T. Kondo⁸², K. Köneke⁵², A.X.Y. Kong¹, A.C. König¹¹⁹, T. Kono¹²⁶, V. Konstantinides⁹⁵, N. Konstantinidis⁹⁵, B. Konya⁹⁷, R. Kopeliansky⁶⁶, S. Koperny^{84a}, K. Korcyl⁸⁵, K. Kordas¹⁶¹, G. Koren¹⁶⁰, A. Korn⁹⁵, I. Korolkov¹⁴, E.V. Korolkova¹⁴⁸, N. Korotkova¹¹³, O. Kortner¹¹⁵, S. Kortner¹¹⁵, V.V. Kostyukhin^{148,165}, A. Kotskechagia⁶⁵, A. Kotwal⁴⁹, A. Koulouris¹⁰, A. Kourkoumeli-Charalampidi^{71a,71b}, C. Kourkoumelis⁹, E. Kourlitis¹⁴⁸, V. Kouskoura²⁹, A.B. Kowalewska⁸⁵, R. Kowalewski¹⁷⁵, W. Kozański¹⁰¹, A.S. Kozhin¹²³, V.A. Kramarenko¹¹³, G. Kramberger⁹², D. Krasnopevtsev^{60a}, M.W. Krasny¹³⁵, A. Krasznahorkay³⁶, D. Krauss¹¹⁵, J.A. Kremer^{84a}, J. Kretzschmar⁹¹, P. Krieger¹⁶⁶, F. Krieter¹¹⁴, A. Krishnan^{61b}, K. Krizka¹⁸, K. Kroeninger⁴⁷, H. Kroha¹¹⁵, J. Kroll¹⁴⁰, J. Kroll¹³⁶, K.S. Krowpman¹⁰⁷, U. Kruchonak⁸⁰, H. Krüger²⁴, N. Krumnack⁷⁹, M.C. Kruse⁴⁹, J.A. Krzysiak⁸⁵, T. Kubota¹⁰⁵, O. Kuchinskaia¹⁶⁵, S. Kuday^{4b}, J.T. Kuechler⁴⁶, S. Kuehn³⁶, A. Kugel^{61a}, T. Kuhl⁴⁶, V. Kukhtin⁸⁰, R. Kukla¹⁰², Y. Kulchitsky^{108,af}, S. Kuleshov^{146b}, Y.P. Kulinich¹⁷², M. Kuna⁵⁸, T. Kunigo⁸⁶, A. Kupco¹⁴⁰, T. Kupfer⁴⁷, O. Kuprash⁵², H. Kurashige⁸³, L.L. Kurchaninov^{167a}, Y.A. Kurochkin¹⁰⁸, A. Kurova¹¹², M.G. Kurth^{15a,15d}, E.S. Kuwertz³⁶, M. Kuze¹⁶⁴, A.K. Kvam¹⁴⁷, J. Kvita¹³⁰, T. Kwan¹⁰⁴, L. La Rotonda^{41b,41a}, F. La Ruffa^{41b,41a}, C. Lacasta¹⁷³, F. Lacava^{73a,73b}, D.P.J. Lack¹⁰¹, H. Lacker¹⁹, D. Lacour¹³⁵, E. Ladygin⁸⁰, R. Lafaye⁵, B. Laforge¹³⁵, T. Lagouri^{146b}, S. Lai⁵³, I.K. Lakomic^{84a}, S. Lammers⁶⁶, W. Lampl⁷, C. Lampoudis¹⁶¹, E. Lançon²⁹, U. Landgraf⁵², M.P.J. Landon⁹³, M.C. Lanfermann⁵⁴, V.S. Lang⁴⁶, J.C. Lange⁵³, R.J. Langenberg¹⁰³, A.J. Lankford¹⁷⁰, F. Lanni²⁹, K. Lantzscheid²⁴, A. Lanza^{71a}, A. Lapertosa^{55b,55a}, S. Laplace¹³⁵, J.F. Laporte¹⁴⁴, T. Lari^{69a}, F. Lasagni Manghi^{23b,23a}, M. Lassnig³⁶, T.S. Lau^{63a}, A. Laudrain⁶⁵, A. Laurier³⁴, M. Lavorgna^{70a,70b}, S.D. Lawlor⁹⁴, M. Lazzaroni^{69a,69b}, B. Le¹⁰¹, E. Le Guirriec¹⁰², A. Lebedev⁷⁹, M. LeBlanc⁷, T. LeCompte⁶, F. Ledroit-Guillon⁵⁸, A.C.A. Lee⁹⁵, C.A. Lee²⁹, G.R. Lee¹⁷, L. Lee⁵⁹, S.C. Lee¹⁵⁷, S. Lee⁷⁹, B. Lefebvre^{167a}, H.P. Lefebvre⁹⁴, M. Lefebvre¹⁷⁵, C. Leggett¹⁸, K. Lehmann¹⁵¹, N. Lehmann²⁰, G. Lehmann Miotto³⁶, W.A. Leight⁴⁶, A. Leisos^{161,v}, M.A.L. Leite^{81d}, C.E. Leitgeb¹¹⁴, R. Leitner¹⁴², D. Lellouch^{179,*}, K.J.C. Leney⁴², T. Lenz²⁴, R. Leone⁷, S. Leone^{72a}, C. Leonidopoulos⁵⁰,

A. Leopold¹³⁵, C. Leroy¹¹⁰, R. Les¹⁶⁶, C.G. Lester³², M. Levchenko¹³⁷, J. Levêque⁵, D. Levin¹⁰⁶, L.J. Levinson¹⁷⁹, D.J. Lewis²¹, B. Li^{15b}, B. Li¹⁰⁶, C.-Q. Li^{60a}, F. Li^{60c}, H. Li^{60a}, H. Li^{60b}, J. Li^{60c}, K. Li¹⁴⁷, L. Li^{60c}, M. Li^{15a,15d}, Q. Li^{15a,15d}, Q.Y. Li^{60a}, S. Li^{60d,60c}, X. Li⁴⁶, Y. Li⁴⁶, Z. Li^{60b}, Z. Li¹⁰⁴, Z. Liang^{15a}, B. Liberti^{74a}, A. Liblong¹⁶⁶, K. Lie^{63c}, S. Lim²⁹, C.Y. Lin³², K. Lin¹⁰⁷, T.H. Lin¹⁰⁰, R.A. Linck⁶⁶, R.E. Lindley⁷, J.H. Lindon²¹, A.L. Lioni⁵⁴, E. Lipeles¹³⁶, A. Lipniacka¹⁷, T.M. Liss^{172,am}, A. Lister¹⁷⁴, J.D. Little⁸, B. Liu⁷⁹, B.L. Liu⁶, H.B. Liu²⁹, H. Liu¹⁰⁶, J.B. Liu^{60a}, J.K.K. Liu³⁷, K. Liu^{60d}, M. Liu^{60a}, P. Liu^{15a}, Y. Liu⁴⁶, Y. Liu^{15a,15d}, Y.L. Liu¹⁰⁶, Y.W. Liu^{60a}, M. Livan^{71a,71b}, A. Lleres⁵⁸, J. Llorente Merino¹⁵¹, S.L. Lloyd⁹³, C.Y. Lo^{63b}, E.M. Lobodzinska⁴⁶, P. Loch⁷, S. Loffredo^{74a,74b}, T. Lohse¹⁹, K. Lohwasser¹⁴⁸, M. Lokajicek¹⁴⁰, J.D. Long¹⁷², R.E. Long⁹⁰, L. Longo³⁶, K.A. Looper¹²⁷, I. Lopez Paz¹⁰¹, A. Lopez Solis¹⁴⁸, J. Lorenz¹¹⁴, N. Lorenzo Martinez⁵, A.M. Lory¹¹⁴, P.J. Lösel¹¹⁴, A. Lösle⁵², X. Lou⁴⁶, X. Lou^{15a}, A. Lounis⁶⁵, J. Love⁶, P.A. Love⁹⁰, J.J. Lozano Bahilo¹⁷³, M. Lu^{60a}, Y.J. Lu⁶⁴, H.J. Lubatti¹⁴⁷, C. Luci^{73a,73b}, A. Lucotte⁵⁸, C. Luedtke⁵², F. Luehring⁶⁶, I. Luise¹³⁵, L. Luminari^{73a}, B. Lund-Jensen¹⁵³, M.S. Lutz¹⁰³, D. Lynn²⁹, H. Lyons⁹¹, R. Lysak¹⁴⁰, E. Lytken⁹⁷, F. Lyu^{15a}, V. Lyubushkin⁸⁰, T. Lyubushkina⁸⁰, H. Ma²⁹, L.L. Ma^{60b}, Y. Ma⁹⁵, G. Maccarrone⁵¹, A. Macchiolo¹¹⁵, C.M. Macdonald¹⁴⁸, J. Machado Miguens¹³⁶, D. Madaffari¹⁷³, R. Madar³⁸, W.F. Mader⁴⁸, M. Madugoda Ralalage Don¹²⁹, N. Madysa⁴⁸, J. Maeda⁸³, T. Maeno²⁹, M. Maerker⁴⁸, V. Magerl⁵², N. Magini⁷⁹, J. Magro^{67a,67c,r}, D.J. Mahon³⁹, C. Maidantchik^{81b}, T. Maier¹¹⁴, A. Maio^{139a,139b,139d}, K. Maj^{84a}, O. Majersky^{28a}, S. Majewski¹³¹, Y. Makida⁸², N. Makovec⁶⁵, B. Malaescu¹³⁵, Pa. Malecki⁸⁵, V.P. Maleev¹³⁷, F. Malek⁵⁸, U. Mallik⁷⁸, D. Malon⁶, C. Malone³², S. Maltezos¹⁰, S. Malyukov⁸⁰, J. Mamuzic¹⁷³, G. Mancini⁵¹, I. Mandić⁹², L. Manhaes de Andrade Filho^{81a}, I.M. Maniatis¹⁶¹, J. Manjarres Ramos⁴⁸, K.H. Mankinen⁹⁷, A. Mann¹¹⁴, A. Manousos⁷⁷, B. Mansoulie¹⁴⁴, I. Manthos¹⁶¹, S. Manzoni¹²⁰, A. Marantis¹⁶¹, G. Marceca³⁰, L. Marchese¹³⁴, G. Marchiori¹³⁵, M. Marcisovsky¹⁴⁰, L. Marcoccia^{74a,74b}, C. Marcon⁹⁷, C.A. Marin Tobon³⁶, M. Marjanovic¹²⁸, Z. Marshall¹⁸, M.U.F. Martensson¹⁷¹, S. Marti-Garcia¹⁷³, C.B. Martin¹²⁷, T.A. Martin¹⁷⁷, V.J. Martin⁵⁰, B. Martin dit Latour¹⁷, L. Martinelli^{75a,75b}, M. Martinez^{14,x}, V.I. Martinez Outschoorn¹⁰³, S. Martin-Haugh¹⁴³, V.S. Martoiu^{27b}, A.C. Martyniuk⁹⁵, A. Marzin³⁶, S.R. Maschek¹¹⁵, L. Masetti¹⁰⁰, T. Mashimo¹⁶², R. Mashinistov¹¹¹, J. Masik¹⁰¹, A.L. Maslennikov^{122b,122a}, L. Massa^{23b,23a}, P. Massarotti^{70a,70b}, P. Mastrandrea^{72a,72b}, A. Mastroberardino^{41b,41a}, T. Masubuchi¹⁶², D. Matakias²⁹, A. Matic¹¹⁴, N. Matsuzawa¹⁶², P. Mättig²⁴, J. Maurer^{27b}, B. Maček⁹², D.A. Maximov^{122b,122a}, R. Mazini¹⁵⁷, I. Maznas¹⁶¹, S.M. Mazza¹⁴⁵, S.P. Mc Kee¹⁰⁶, T.G. McCarthy¹¹⁵, W.P. McCormack¹⁸, E.F. McDonald¹⁰⁵, J.A. Mcfayden³⁶, G. Mchedlidze^{158b}, M.A. McKay⁴², K.D. McLean¹⁷⁵, S.J. McMahon¹⁴³, P.C. McNamara¹⁰⁵, C.J. McNicol¹⁷⁷, R.A. McPherson^{175,ac}, J.E. Mdhluli^{33e}, Z.A. Meadows¹⁰³, S. Meehan³⁶, T. Megy³⁸, S. Mehlhase¹¹⁴, A. Mehta⁹¹, T. Meideck⁵⁸, B. Meirose⁴³, D. Melini¹⁵⁹, B.R. Mellado Garcia^{33e}, J.D. Mellenthin⁵³, M. Melo^{28a}, F. Meloni⁴⁶, A. Melzer²⁴, S.B. Menary¹⁰¹, E.D. Mendes Gouveia^{139a,139e}, L. Meng³⁶, X.T. Meng¹⁰⁶, S. Menke¹¹⁵, E. Meoni^{41b,41a}, S. Mergelmeyer¹⁹, S.A.M. Merkt¹³⁸, C. Merlassino¹³⁴, P. Mermod⁵⁴, L. Merola^{70a,70b}, C. Meroni^{69a}, G. Merz¹⁰⁶, O. Meshkov^{113,111}, J.K.R. Meshreki¹⁵⁰, A. Messina^{73a,73b}, J. Metcalfe⁶, A.S. Mete⁶, C. Meyer⁶⁶, J.-P. Meyer¹⁴⁴, H. Meyer Zu Theenhausen^{61a}, F. Miano¹⁵⁵, M. Michetti¹⁹, R.P. Middleton¹⁴³, L. Mijović⁵⁰, G. Mikenberg¹⁷⁹, M. Mikestikova¹⁴⁰, M. Mikuž⁹², H. Mildner¹⁴⁸, M. Milesi¹⁰⁵, A. Milic¹⁶⁶, C.D. Milke⁴², D.W. Miller³⁷, A. Milov¹⁷⁹, D.A. Milstead^{45a,45b}, R.A. Mina¹⁵², A.A. Minaenko¹²³, M. Miñano Moya¹⁷³, I.A. Minashvili^{158b}, A.I. Mincer¹²⁵, B. Mindur^{84a}, M. Mineev⁸⁰, Y. Minegishi¹⁶², L.M. Mir¹⁴, A. Mirto^{68a,68b}, K.P. Mistry¹³⁶, T. Mitani¹⁷⁸, J. Mitrevski¹¹⁴, V.A. Mitsou¹⁷³, M. Mittal^{60c}, O. Miu¹⁶⁶, A. Miucci²⁰, P.S. Miyagawa¹⁴⁸, A. Mizukami⁸², J.U. Mjörnmark⁹⁷, T. Mkrtchyan^{61a}, M. Mlynarikova¹⁴², T. Moa^{45a,45b}, K. Mochizuki¹¹⁰, P. Mogg¹¹⁴, S. Mohapatra³⁹, R. Moles-Valls²⁴, M.C. Mondragon¹⁰⁷, K. Mönig⁴⁶, J. Monk⁴⁰, E. Monnier¹⁰², A. Montalbano¹⁵¹, J. Montejo Berlingen³⁶, M. Montella⁹⁵, F. Monticelli⁸⁹, S. Monzani^{69a}, N. Morange⁶⁵, D. Moreno^{22a}, M. Moreno Llácer¹⁷³, C. Moreno Martinez¹⁴, P. Morettini^{55b}, M. Morgenstern¹⁵⁹, S. Morgenstern⁴⁸, D. Mori¹⁵¹, M. Morii⁵⁹, M. Morinaga¹⁷⁸, V. Morisbak¹³³, A.K. Morley³⁶, G. Mornacchi³⁶, A.P. Morris⁹⁵, L. Morvaj¹⁵⁴, P. Moschovakos³⁶, B. Moser¹²⁰, M. Mosidze^{158b}, T. Moskalets¹⁴⁴, H.J. Moss¹⁴⁸, J. Moss^{31,m}, E.J.W. Moyse¹⁰³, S. Muanza¹⁰², J. Mueller¹³⁸, R.S.P. Mueller¹¹⁴, D. Muenstermann⁹⁰, G.A. Mullier⁹⁷, D.P. Mungo^{69a,69b}, J.L. Munoz Martinez¹⁴, F.J. Munoz Sanchez¹⁰¹, P. Murin^{28b}, W.J. Murray^{177,143}, A. Murrone^{69a,69b}, M. Muškinja¹⁸, C. Mwewa^{33a}, A.G. Myagkov^{123,ah}, A.A. Myers¹³⁸, J. Myers¹³¹, M. Myska¹⁴¹, B.P. Nachman¹⁸, O. Nackenhorst⁴⁷, A. Nag Nag⁴⁸, K. Nagai¹³⁴, K. Nagano⁸²,

Y. Nagasaka⁶², J.L. Nagle²⁹, E. Nagy¹⁰², A.M. Nairz³⁶, Y. Nakahama¹¹⁷, K. Nakamura⁸², T. Nakamura¹⁶², H. Nanjo¹³², F. Napolitano^{61a}, R.F. Naranjo Garcia⁴⁶, R. Narayan⁴², I. Naryshkin¹³⁷, T. Naumann⁴⁶, G. Navarro^{22a}, P.Y. Nechaeva¹¹¹, F. Nechansky⁴⁶, T.J. Neep²¹, A. Negri^{71a,71b}, M. Negrini^{23b}, C. Nellist¹¹⁹, M.E. Nelson^{45a,45b}, S. Nemecek¹⁴⁰, M. Nessi^{36,d}, M.S. Neubauer¹⁷², F. Neuhaus¹⁰⁰, M. Neumann¹⁸¹, R. Newhouse¹⁷⁴, P.R. Newman²¹, C.W. Ng¹³⁸, Y.S. Ng¹⁹, Y.W.Y. Ng¹⁷⁰, B. Ngair^{35e}, H.D.N. Nguyen¹⁰², T. Nguyen Manh¹¹⁰, E. Nibigira³⁸, R.B. Nickerson¹³⁴, R. Nicolaidou¹⁴⁴, D.S. Nielsen⁴⁰, J. Nielsen¹⁴⁵, N. Nikiforou¹¹, V. Nikolaenko^{123,ah}, I. Nikolic-Audit¹³⁵, K. Nikolopoulos²¹, P. Nilsson²⁹, H.R. Nindhito⁵⁴, Y. Ninomiya⁸², A. Nisati^{73a}, N. Nishu^{60c}, R. Nisius¹¹⁵, I. Nitsche⁴⁷, T. Nitta¹⁷⁸, T. Nobe¹⁶², Y. Noguchi⁸⁶, I. Nomidis¹³⁵, M.A. Nomura²⁹, M. Nordberg³⁶, T. Novak⁹², O. Novgorodova⁴⁸, R. Novotny¹⁴¹, L. Nozka¹³⁰, K. Ntekas¹⁷⁰, E. Nurse⁹⁵, F.G. Oakham^{34,an}, H. Oberlack¹¹⁵, J. Ocariz¹³⁵, A. Ochi⁸³, I. Ochoa³⁹, J.P. Ochoa-Ricoux^{146a}, K. O'Connor²⁶, S. Oda⁸⁸, S. Odaka⁸², S. Oerdek⁵³, A. Ogrodnik^{84a}, A. Oh¹⁰¹, S.H. Oh⁴⁹, C.C. Ohm¹⁵³, H. Oide¹⁶⁴, M.L. Ojeda¹⁶⁶, H. Okawa¹⁶⁸, Y. Okazaki⁸⁶, M.W. O'Keefe⁹¹, Y. Okumura¹⁶², T. Okuyama⁸², A. Olariu^{27b}, L.F. Oleiro Seabra^{139a}, S.A. Olivares Pino^{146a}, D. Oliveira Damazio²⁹, J.L. Oliver¹, M.J.R. Olsson¹⁷⁰, A. Olszewski⁸⁵, J. Olszowska⁸⁵, D.C. O'Neil¹⁵¹, A.P. O'Neill¹³⁴, A. Onofre^{139a,139e}, P.U.E. Onyisi¹¹, H. Oppen¹³³, M.J. Oreglia³⁷, G.E. Orellana⁸⁹, D. Orestano^{75a,75b}, N. Orlando¹⁴, R.S. Orr¹⁶⁶, V. O'Shea⁵⁷, R. Ospanov^{60a}, G. Otero y Garzon³⁰, H. Otono⁸⁸, P.S. Ott^{61a}, G.J. Ottino¹⁸, M. Ouchrif^{35d}, J. Ouellette²⁹, F. Ould-Saada¹³³, A. Ouraou¹⁴⁴, Q. Ouyang^{15a}, M. Owen⁵⁷, R.E. Owen²¹, V.E. Ozcan^{12c}, N. Ozturk⁸, J. Pacalt¹³⁰, H.A. Pacey³², K. Pachal⁴⁹, A. Pacheco Pages¹⁴, C. Padilla Aranda¹⁴, S. Pagan Griso¹⁸, M. Paganini¹⁸², G. Palacino⁶⁶, S. Palazzo⁵⁰, S. Palestini³⁶, M. Palka^{84b}, D. Pallin³⁸, P. Palni^{84a}, I. Panagoulas¹⁰, C.E. Pandini³⁶, J.G. Panduro Vazquez⁹⁴, P. Pani⁴⁶, G. Panizzo^{67a,67c}, L. Paolozzi⁵⁴, C. Papadatos¹¹⁰, K. Papageorgiou^{9,g}, S. Parajuli⁴², A. Paramonov⁶, D. Paredes Hernandez^{63b}, S.R. Paredes Saenz¹³⁴, B. Parida¹⁶⁵, T.H. Park¹⁶⁶, A.J. Parker³¹, M.A. Parker³², F. Parodi^{55b,55a}, E.W. Parrish¹²¹, J.A. Parsons³⁹, U. Parzefall⁵², L. Pascual Dominguez¹³⁵, V.R. Pascuzzi¹⁸, J.M.P. Pasner¹⁴⁵, F. Pasquali¹²⁰, E. Pasqualucci^{73a}, S. Passaggio^{55b}, F. Pastore⁹⁴, P. Pasuwan^{45a,45b}, S. Patariaia¹⁰⁰, J.R. Pater¹⁰¹, A. Pathak^{180,i}, J. Patton⁹¹, T. Pauly³⁶, J. Pearkes¹⁵², B. Pearson¹¹⁵, M. Pedersen¹³³, L. Pedraza Diaz¹¹⁹, R. Pedro^{139a}, T. Peiffer⁵³, S.V. Peleganchuk^{122b,122a}, O. Penc¹⁴⁰, H. Peng^{60a}, B.S. Peralva^{81a}, M.M. Perego⁶⁵, A.P. Pereira Peixoto^{139a}, L. Pereira Sanchez^{45a,45b}, D.V. Perepelitsa²⁹, F. Peri¹⁹, L. Perini^{69a,69b}, H. Pernegger³⁶, S. Perrella^{139a}, A. Perrevoort¹²⁰, K. Peters⁴⁶, R.F.Y. Peters¹⁰¹, B.A. Petersen³⁶, T.C. Petersen⁴⁰, E. Petit¹⁰², A. Petridis¹, C. Petridou¹⁶¹, P. Petroff⁶⁵, F. Petrucci^{75a,75b}, M. Pettee¹⁸², N.E. Pettersson¹⁰³, K. Petukhova¹⁴², A. Peyaud¹⁴⁴, R. Pezoa^{146d}, L. Pezzotti^{71a,71b}, T. Pham¹⁰⁵, F.H. Phillips¹⁰⁷, P.W. Phillips¹⁴³, M.W. Phipps¹⁷², G. Piacquadio¹⁵⁴, E. Pianori¹⁸, A. Picazio¹⁰³, R.H. Pickles¹⁰¹, R. Piegaia³⁰, D. Pietreanu^{27b}, J.E. Pilcher³⁷, A.D. Pilkington¹⁰¹, M. Pinamonti^{67a,67c}, J.L. Pinfold³, C. Pitman Donaldson⁹⁵, M. Pitt¹⁶⁰, L. Pizzimento^{74a,74b}, M.-A. Pleier²⁹, V. Pleskot¹⁴², E. Plotnikova⁸⁰, P. Podberezko^{122b,122a}, R. Poettgen⁹⁷, R. Poggi⁵⁴, L. Poggioli¹³⁵, I. Pogrebnyak¹⁰⁷, D. Pohl²⁴, I. Pokharel⁵³, G. Polesello^{71a}, A. Poley¹⁸, A. Policicchio^{73a,73b}, R. Polifka¹⁴², A. Polini^{23b}, C.S. Pollard⁴⁶, V. Polychronakos²⁹, D. Ponomarenko¹¹², L. Pontecorvo³⁶, S. Popa^{27a}, G.A. Popeneciu^{27d}, L. Portales⁵, D.M. Portillo Quintero⁵⁸, S. Pospisil¹⁴¹, K. Potamianos⁴⁶, I.N. Potrap⁸⁰, C.J. Potter³², H. Potti¹¹, T. Poulsen⁹⁷, J. Poveda³⁶, T.D. Powell¹⁴⁸, G. Pownall⁴⁶, M.E. Pozo Astigarraga³⁶, P. Pralavorio¹⁰², S. Prell⁷⁹, D. Price¹⁰¹, M. Primavera^{68a}, S. Prince¹⁰⁴, M.L. Proffitt¹⁴⁷, N. Proklova¹¹², K. Prokofiev^{63c}, F. Prokoshin⁸⁰, S. Protopopescu²⁹, J. Proudfoot⁶, M. Przybycien^{84a}, D. Pudza¹³⁷, A. Puri¹⁷², P. Puzo⁶⁵, J. Qian¹⁰⁶, Y. Qin¹⁰¹, A. Quadt⁵³, M. Queitsch-Maitland³⁶, A. Qureshi¹, M. Racko^{28a}, F. Ragusa^{69a,69b}, G. Rahal⁹⁸, J.A. Raine⁵⁴, S. Rajagopalan²⁹, A. Ramirez Morales⁹³, K. Ran^{15a,15d}, T. Rashid⁶⁵, S. Raspopov⁵, D.M. Rauch⁴⁶, F. Rauscher¹¹⁴, S. Rave¹⁰⁰, B. Ravina¹⁴⁸, I. Ravinovich¹⁷⁹, J.H. Rawling¹⁰¹, M. Raymond³⁶, A.L. Read¹³³, N.P. Readioff⁵⁸, M. Reale^{68a,68b}, D.M. Rebuffi^{71a,71b}, G. Redlinger²⁹, K. Reeves⁴³, L. Rehnisch¹⁹, J. Reichert¹³⁶, D. Reikher¹⁶⁰, A. Reiss¹⁰⁰, A. Rej¹⁵⁰, C. Rembser³⁶, A. Renardi⁴⁶, M. Renda^{27b}, M. Rescigno^{73a}, S. Resconi^{69a}, E.D. Resseguie¹⁸, S. Rettie⁹⁵, B. Reynolds¹²⁷, E. Reynolds²¹, O.L. Rezanova^{122b,122a}, P. Reznicek¹⁴², E. Ricci^{76a,76b}, R. Richter¹¹⁵, S. Richter⁴⁶, E. Richter-Was^{84b}, O. Ricken²⁴, M. Ridel¹³⁵, P. Rieck¹¹⁵, O. Rifki⁴⁶, M. Rijssenbeek¹⁵⁴, A. Rimoldi^{71a,71b}, M. Rimoldi⁴⁶, L. Rinaldi^{23b}, G. Ripellino¹⁵³, I. Riu¹⁴, J.C. Rivera Vergara¹⁷⁵, F. Rizatdinova¹²⁹, E. Rizvi⁹³, C. Rizzi³⁶, R.T. Roberts¹⁰¹, S.H. Robertson^{104,ac}, M. Robin⁴⁶, D. Robinson³², C.M. Robles Gajardo^{146d}, M. Robles Manzano¹⁰⁰, A. Robson⁵⁷, A. Rocchi^{74a,74b}, E. Rocco¹⁰⁰, C. Roda^{72a,72b}, S. Rodriguez Bosca¹⁷³,

A. Rodríguez Perez¹⁴, D. Rodríguez Rodríguez¹⁷³, A.M. Rodríguez Vera^{167b}, S. Roe³⁶, O. Røhne¹³³, R. Röhrig¹¹⁵, R.A. Rojas^{146d}, B. Roland⁵², C.P.A. Roland⁶⁶, J. Roloff²⁹, A. Romaniouk¹¹², M. Romano^{23b,23a}, N. Rompotis⁹¹, M. Ronzani¹²⁵, L. Roos¹³⁵, S. Rosati^{73a}, G. Rosin¹⁰³, B.J. Rosser¹³⁶, E. Rossi⁴⁶, E. Rossi^{75a,75b}, E. Rossi^{70a,70b}, L.P. Rossi^{55b}, L. Rossini^{69a,69b}, R. Rosten¹⁴, M. Rotaru^{27b}, B. Rottler⁵², D. Rousseau⁶⁵, G. Rovelli^{71a,71b}, A. Roy¹¹, D. Roy^{33e}, A. Rozanov¹⁰², Y. Rozen¹⁵⁹, X. Ruan^{33e}, F. Rühr⁵², A. Ruiz-Martinez¹⁷³, A. Rummler³⁶, Z. Rurikova⁵², N.A. Rusakovich⁸⁰, H.L. Russell¹⁰⁴, L. Rustige^{38,47}, J.P. Rutherford⁷, E.M. Rüttinger¹⁴⁸, M. Rybar³⁹, G. Rybkin⁶⁵, E.B. Rye¹³³, A. Ryzhov¹²³, J.A. Sabater Iglesias⁴⁶, P. Sabatini⁵³, S. Sacerdoti⁶⁵, H.F.-W. Sadrozinski¹⁴⁵, R. Sadykov⁸⁰, F. Safai Tehrani^{73a}, B. Safarzadeh Samani¹⁵⁵, M. Safdari¹⁵², P. Saha¹²¹, S. Saha¹⁰⁴, M. Sahinsoy^{61a}, A. Sahu¹⁸¹, M. Saimpert³⁶, M. Saito¹⁶², T. Saito¹⁶², H. Sakamoto¹⁶², D. Salamani⁵⁴, G. Salamanna^{75a,75b}, J.E. Salazar Loyola^{146d}, A. Salnikov¹⁵², J. Salt¹⁷³, A. Salvador Salas¹⁴, D. Salvatore^{41b,41a}, F. Salvatore¹⁵⁵, A. Salvucci^{63a,63b,63c}, A. Salzburger³⁶, J. Samarati³⁶, D. Sammel⁵², D. Sampsonidis¹⁶¹, D. Sampsonidou¹⁶¹, J. Sánchez¹⁷³, A. Sanchez Pineda^{67a,36,67c}, H. Sandaker¹³³, C.O. Sander⁴⁶, I.G. Sanderswood⁹⁰, M. Sandhoff¹⁸¹, C. Sandoval^{22a}, D.P.C. Sankey¹⁴³, M. Sannino^{55b,55a}, Y. Sano¹¹⁷, A. Sansoni⁵¹, C. Santoni³⁸, H. Santos^{139a,139b}, S.N. Santpur¹⁸, A. Santra¹⁷³, A. Saproinov⁸⁰, J.G. Saraiva^{139a,139d}, O. Sasaki⁸², K. Sato¹⁶⁸, F. Sauerburger⁵², E. Sauvan⁵, P. Savard^{166,an}, R. Sawada¹⁶², C. Sawyer¹⁴³, L. Sawyer^{96,ag}, C. Sbarra^{23b}, A. Sbrizzi^{23a}, T. Scanlon⁹⁵, J. Schaarschmidt¹⁴⁷, P. Schacht¹¹⁵, B.M. Schachtner¹¹⁴, D. Schaefer³⁷, L. Schaefer¹³⁶, J. Schaeffer¹⁰⁰, S. Schaepe³⁶, U. Schäfer¹⁰⁰, A.C. Schaffer⁶⁵, D. Schaile¹¹⁴, R.D. Schamberger¹⁵⁴, N. Scharmberg¹⁰¹, V.A. Schegelsky¹³⁷, D. Scheirich¹⁴², F. Schenck¹⁹, M. Schernau¹⁷⁰, C. Schiavi^{55b,55a}, L.K. Schildgen²⁴, Z.M. Schillaci²⁶, E.J. Schioppa^{68a,68b}, M. Schioppa^{41b,41a}, K.E. Schleicher⁵², S. Schlenker³⁶, K.R. Schmidt-Sommerfeld¹¹⁵, K. Schmieden³⁶, C. Schmitt¹⁰⁰, S. Schmitt⁴⁶, S. Schmitz¹⁰⁰, J.C. Schmoeckel⁴⁶, L. Schoeffel¹⁴⁴, A. Schoening^{61b}, P.G. Scholer⁵², E. Schopf¹³⁴, M. Schott¹⁰⁰, J.F.P. Schouwenberg¹¹⁹, J. Schovancova³⁶, S. Schramm⁵⁴, F. Schroeder¹⁸¹, A. Schulte¹⁰⁰, H.-C. Schultz-Coulon^{61a}, M. Schumacher⁵², B.A. Schumm¹⁴⁵, Ph. Schune¹⁴⁴, A. Schwartzman¹⁵², T.A. Schwarz¹⁰⁶, Ph. Schwemling¹⁴⁴, R. Schwienhorst¹⁰⁷, A. Sciandra¹⁴⁵, G. Sciolla²⁶, M. Scodeggio⁴⁶, M. Scornajenghi^{41b,41a}, F. Scuri^{72a}, F. Scutti¹⁰⁵, L.M. Scyboz¹¹⁵, C.D. Sebastiani^{73a,73b}, P. Seema¹⁹, S.C. Seidel¹¹⁸, A. Seiden¹⁴⁵, B.D. Seidlitz²⁹, T. Seiss³⁷, C. Seitz⁴⁶, J.M. Seixas^{81b}, G. Sekhniaidze^{70a}, S.J. Sekula⁴², N. Semprini-Cesari^{23b,23a}, S. Sen⁴⁹, C. Serfon⁷⁷, L. Serin⁶⁵, L. Serkin^{67a,67b}, M. Sessa^{60a}, H. Severini¹²⁸, S. Sevova¹⁵², F. Sforza^{55b,55a}, A. Sfyrla⁵⁴, E. Shabalina⁵³, J.D. Shahinian¹⁴⁵, N.W. Shaikh^{45a,45b}, D. Shaked Renous¹⁷⁹, L.Y. Shan^{15a}, M. Shapiro¹⁸, A. Sharma¹³⁴, A.S. Sharma¹, P.B. Shatalov¹²⁴, K. Shaw¹⁵⁵, S.M. Shaw¹⁰¹, M. Shehade¹⁷⁹, Y. Shen¹²⁸, A.D. Sherman²⁵, P. Sherwood⁹⁵, L. Shi¹⁵⁷, S. Shimizu⁸², C.O. Shimmin¹⁸², Y. Shimogama¹⁷⁸, M. Shimojima¹¹⁶, I.P.J. Shipsey¹³⁴, S. Shirabe¹⁶⁴, M. Shiyakova^{80,aa}, J. Shlomi¹⁷⁹, A. Shmeleva¹¹¹, M.J. Shochet³⁷, J. Shojaii¹⁰⁵, D.R. Shope¹²⁸, S. Shrestha¹²⁷, E.M. Shrif^{33e}, E. Shulga¹⁷⁹, P. Sicho¹⁴⁰, A.M. Sickles¹⁷², P.E. Sidebo¹⁵³, E. Sideras Haddad^{33e}, O. Sidiropoulou³⁶, A. Sidoti^{23b,23a}, F. Siegert⁴⁸, Dj. Sijacki¹⁶, M.Jr. Silva¹⁸⁰, M.V. Silva Oliveira^{81a}, S.B. Silverstein^{45a}, S. Simion⁶⁵, R. Simoniello¹⁰⁰, C.J. Simpson-allso²¹, S. Simsek^{12b}, P. Sinervo¹⁶⁶, V. Sinetckii¹¹³, S. Singh¹⁵¹, M. Sioli^{23b,23a}, I. Siral¹³¹, S.Yu. Sivoklokov¹¹³, J. Sjölin^{45a,45b}, E. Skorda⁹⁷, P. Skubic¹²⁸, M. Slawinska⁸⁵, K. Sliwa¹⁶⁹, R. Slovak¹⁴², V. Smakhtin¹⁷⁹, B.H. Smart¹⁴³, J. Smiesko^{28b}, N. Smirnov¹¹², S.Yu. Smirnov¹¹², Y. Smirnov¹¹², L.N. Smirnova^{113,s}, O. Smirnova⁹⁷, J.W. Smith⁵³, M. Smizanska⁹⁰, K. Smolek¹⁴¹, A. Smykiewicz⁸⁵, A.A. Snesarev¹¹¹, H.L. Snoek¹²⁰, I.M. Snyder¹³¹, S. Snyder²⁹, R. Sobie^{175,ac}, A. Soffer¹⁶⁰, A. Søgaard⁵⁰, F. Sohns⁵³, C.A. Solans Sanchez³⁶, E.Yu. Soldatov¹¹², U. Soldevila¹⁷³, A.A. Solodkov¹²³, A. Soloshenko⁸⁰, O.V. Solovyanov¹²³, V. Solov'yev¹³⁷, P. Sommer¹⁴⁸, H. Son¹⁶⁹, W. Song¹⁴³, W.Y. Song^{167b}, A. Sopczak¹⁴¹, A.L. Sopio⁹⁵, F. Sopkova^{28b}, C.L. Sotiropoulou^{72a,72b}, S. Sottocornola^{71a,71b}, R. Soualah^{67a,67c,f}, A.M. Soukharev^{122b,122a}, D. South⁴⁶, S. Spagnolo^{68a,68b}, M. Spalla¹¹⁵, M. Spangenberg¹⁷⁷, F. Spanò⁹⁴, D. Sperlich⁵², T.M. Spieker^{61a}, G. Spigo³⁶, M. Spina¹⁵⁵, D.P. Spiteri⁵⁷, M. Spousta¹⁴², A. Stabile^{69a,69b}, B.L. Stamas¹²¹, R. Stamen^{61a}, M. Stamenkovic¹²⁰, E. Stanecka⁸⁵, B. Stanislaus¹³⁴, M.M. Stanitzki⁴⁶, M. Stankaityte¹³⁴, B. Stapf¹²⁰, E.A. Starchenko¹²³, G.H. Stark¹⁴⁵, J. Stark⁵⁸, P. Staroba¹⁴⁰, P. Starovoitov^{61a}, S. Stärz¹⁰⁴, R. Staszewski⁸⁵, G. Stavropoulos⁴⁴, M. Stegler⁴⁶, P. Steinberg²⁹, A.L. Steinhebel¹³¹, B. Stelzer¹⁵¹, H.J. Stelzer¹³⁸, O. Stelzer-Chilton^{167a}, H. Stenzel⁵⁶, T.J. Stevenson¹⁵⁵, G.A. Stewart³⁶, M.C. Stockton³⁶, G. Stoica^{27b}, M. Stolarski^{139a}, S. Stonjek¹¹⁵, A. Straessner⁴⁸, J. Strandberg¹⁵³, S. Strandberg^{45a,45b}, M. Strauss¹²⁸, P. Strizenec^{28b}, R. Ströhmer¹⁷⁶, D.M. Strom¹³¹,

R. Stroyanowski⁴², A. Strubig⁵⁰, S.A. Stucci²⁹, B. Stugu¹⁷, J. Stupak¹²⁸, N.A. Styles⁴⁶, D. Su¹⁵², W. Su^{60c}, S. Suchek^{61a}, V.V. Sulin¹¹¹, M.J. Sullivan⁹¹, D.M.S. Sultan⁵⁴, S. Sultansoy^{4c}, T. Sumida⁸⁶, S. Sun¹⁰⁶, X. Sun¹⁰¹, K. Suruliz¹⁵⁵, C.J.E. Suster¹⁵⁶, M.R. Sutton¹⁵⁵, S. Suzuki⁸², M. Svatos¹⁴⁰, M. Swiatkowski^{167a}, S.P. Swift², T. Swirski¹⁷⁶, A. Sydorenko¹⁰⁰, I. Sykora^{28a}, M. Sykora¹⁴², T. Sykora¹⁴², D. Ta¹⁰⁰, K. Tackmann^{46,y}, J. Taenzer¹⁶⁰, A. Taffard¹⁷⁰, R. Tafirout^{167a}, R. Takashima⁸⁷, K. Takeda⁸³, T. Takeshita¹⁴⁹, E.P. Takeva⁵⁰, Y. Takubo⁸², M. Talby¹⁰², A.A. Talyshev^{122b,122a}, N.M. Tamir¹⁶⁰, J. Tanaka¹⁶², R. Tanaka⁶⁵, S. Tapia Araya¹⁷², S. Tapprogge¹⁰⁰, A. Tarek Abouelfadl Mohamed¹⁰⁷, S. Tarem¹⁵⁹, K. Tariq^{60b}, G. Tarna^{27b,c}, G.F. Tartarelli^{69a}, P. Tas¹⁴², M. Tasevsky¹⁴⁰, T. Tashiro⁸⁶, E. Tassi^{41b,41a}, A. Tavares Delgado^{139a}, Y. Tayalati^{35e}, A.J. Taylor⁵⁰, G.N. Taylor¹⁰⁵, W. Taylor^{167b}, H. Teagle⁹¹, A.S. Tee⁹⁰, R. Teixeira De Lima¹⁵², P. Teixeira-Dias⁹⁴, H. Ten Kate³⁶, J.J. Teoh¹²⁰, S. Terada⁸², K. Terashi¹⁶², J. Terron⁹⁹, S. Terzo¹⁴, M. Testa⁵¹, R.J. Teuscher^{166,ac}, S.J. Thais¹⁸², N. Themistokleous⁵⁰, T. Theveneaux-Pelzer⁴⁶, F. Thiele⁴⁰, D.W. Thomas⁹⁴, J.O. Thomas⁴², J.P. Thomas²¹, P.D. Thompson²¹, L.A. Thomsen¹⁸², E. Thomson¹³⁶, E.J. Thorpe⁹³, R.E. Ticse Torres⁵³, V.O. Tikhomirov^{111,ai}, Yu.A. Tikhonov^{122b,122a}, S. Timoshenko¹¹², P. Tipton¹⁸², S. Tisserant¹⁰², K. Todome^{23b,23a}, S. Todorova-Nova¹⁴², S. Todt⁴⁸, J. Tojo⁸⁸, S. Tokár^{28a}, K. Tokushuku⁸², E. Tolley¹²⁷, K.G. Tomiwa^{33e}, M. Tomoto¹¹⁷, L. Tompkins¹⁵², P. Tornambe¹⁰³, E. Torrence¹³¹, H. Torres⁴⁸, E. Torró Pastor¹⁴⁷, C. Toscirì¹³⁴, J. Toth^{102,ab}, D.R. Tovey¹⁴⁸, A. Traeet¹⁷, C.J. Treado¹²⁵, T. Trefzger¹⁷⁶, F. Tresoldi¹⁵⁵, A. Tricoli²⁹, I.M. Trigger^{167a}, S. Trincaz-Duvioi¹³⁵, D.A. Trischuk¹⁷⁴, W. Trischuk¹⁶⁶, B. Trocmé⁵⁸, A. Trofymov¹⁴⁴, C. Troncon^{69a}, F. Trovato¹⁵⁵, L. Truong^{33c}, M. Trzebinski⁸⁵, A. Trzupek⁸⁵, F. Tsai⁴⁶, J.C.-L. Tseng¹³⁴, P.V. Tsiarehsha^{108,af}, A. Tsirigotis^{161,v}, V. Tsiskaridze¹⁵⁴, E.G. Tskhadadze^{158a}, M. Tsopoulou¹⁶¹, I.I. Tsukerman¹²⁴, V. Tsulaia¹⁸, S. Tsuno⁸², D. Tsybychev¹⁵⁴, Y. Tu^{63b}, A. Tudorache^{27b}, V. Tudorache^{27b}, T.T. Tulbure^{27a}, A.N. Tuna⁵⁹, S. Turchikhin⁸⁰, D. Turgeman¹⁷⁹, I. Turk Cakir^{4b,t}, R.J. Turner²¹, R.T. Turra^{69a}, P.M. Tuts³⁹, S. Tzamarias¹⁶¹, E. Tzovara¹⁰⁰, G. Ucchielli⁴⁷, K. Uchida¹⁶², F. Ukegawa¹⁶⁸, G. Unal³⁶, A. Undrus²⁹, G. Unel¹⁷⁰, F.C. Ungaro¹⁰⁵, Y. Unno⁸², K. Uno¹⁶², J. Urban^{28b}, P. Urquijo¹⁰⁵, G. Usai⁸, Z. Uysal^{12d}, V. Vacek¹⁴¹, B. Vachon¹⁰⁴, K.O.H. Vadla¹³³, A. Vaidya⁹⁵, C. Valderanis¹¹⁴, E. Valdes Santurio^{45a,45b}, M. Valente⁵⁴, S. Valentini^{23b,23a}, A. Valero¹⁷³, L. Valéry⁴⁶, R.A. Vallance²¹, A. Vallier³⁶, J.A. Valls Ferrer¹⁷³, T.R. Van Daalen¹⁴, P. Van Gemmeren⁶, I. Van Vulpen¹²⁰, M. Vanadia^{74a,74b}, W. Vandelli³⁶, M. Vandenbroucke¹⁴⁴, E.R. Vandewall¹²⁹, A. Vaniachine¹⁶⁵, D. Vannicola^{73a,73b}, R. Vari^{73a}, E.W. Varnes⁷, C. Varni^{55b,55a}, T. Varol¹⁵⁷, D. Varouchas⁶⁵, K.E. Varvell¹⁵⁶, M.E. Vasile^{27b}, G.A. Vasquez¹⁷⁵, F. Vazeille³⁸, D. Vazquez Furelos¹⁴, T. Vazquez Schroeder³⁶, J. Veatch⁵³, V. Vecchio^{75a,75b}, M.J. Veen¹²⁰, L.M. Veloce¹⁶⁶, F. Veloso^{139a,139c}, S. Veneziano^{73a}, A. Ventura^{68a,68b}, N. Venturi³⁶, A. Verbitskyi¹¹⁵, V. Vercesi^{71a}, M. Verducci^{72a,72b}, C.M. Vergel Infante⁷⁹, C. Vergis²⁴, W. Verkerke¹²⁰, A.T. Vermeulen¹²⁰, J.C. Vermeulen¹²⁰, C. Vernieri¹⁵², M.C. Vetterli^{151,an}, N. Viaux Maira^{146d}, T. Vickey¹⁴⁸, O.E. Vickey Boeriu¹⁴⁸, G.H.A. Viehhauser¹³⁴, L. Vigani^{61b}, M. Villa^{23b,23a}, M. Villaplana Perez³, E. Vilucchi⁵¹, M.G. Vinciter³⁴, G.S. Virdee²¹, A. Vishwakarma⁴⁶, C. Vittori^{23b,23a}, I. Vivarelli¹⁵⁵, M. Vogel¹⁸¹, P. Vokac¹⁴¹, S.E. von Buddenbrock^{33e}, E. Von Toerne²⁴, V. Vorobel¹⁴², K. Vorobev¹¹², M. Vos¹⁷³, J.H. Vosseveld⁹¹, M. Vozak¹⁰¹, N. Vranjes¹⁶, M. Vranjes Milosavljevic¹⁶, V. Vrba¹⁴¹, M. Vreeswijk¹²⁰, R. Vuillermet³⁶, I. Vukotic³⁷, S. Wada¹⁶⁸, P. Wagner²⁴, W. Wagner¹⁸¹, J. Wagner-Kuhr¹¹⁴, S. Wahdan¹⁸¹, H. Wahlberg⁸⁹, R. Wakasa¹⁶⁸, V.M. Walbrecht¹¹⁵, J. Walder⁹⁰, R. Walker¹¹⁴, S.D. Walker⁹⁴, W. Walkowiak¹⁵⁰, V. Wallangen^{45a,45b}, A.M. Wang⁵⁹, A.Z. Wang¹⁸⁰, C. Wang^{60c}, F. Wang¹⁸⁰, H. Wang¹⁸, H. Wang³, J. Wang^{63a}, J. Wang^{61b}, P. Wang⁴², Q. Wang¹²⁸, R.-J. Wang¹⁰⁰, R. Wang^{60a}, R. Wang⁶, S.M. Wang¹⁵⁷, W.T. Wang^{60a}, W. Wang^{15c}, W.X. Wang^{60a}, Y. Wang^{60a}, Z. Wang^{60c}, C. Wanotayaroj⁴⁶, A. Warburton¹⁰⁴, C.P. Ward³², D.R. Wardrope⁹⁵, N. Warrack⁵⁷, A. Washbrook⁵⁰, A.T. Watson²¹, M.F. Watson²¹, G. Watts¹⁴⁷, B.M. Waugh⁹⁵, A.F. Webb¹¹, C. Weber¹⁸², M.S. Weber²⁰, S.A. Weber³⁴, S.M. Weber^{61a}, A.R. Weidberg¹³⁴, J. Weingarten⁴⁷, M. Weirich¹⁰⁰, C. Weiser⁵², P.S. Wells³⁶, T. Wenaus²⁹, T. Wengler³⁶, S. Wenig³⁶, N. Wermes²⁴, M.D. Werner⁷⁹, M. Wessels^{61a}, T.D. Weston²⁰, K. Whalen¹³¹, N.L. Whallon¹⁴⁷, A.M. Wharton⁹⁰, A.S. White¹⁰⁶, A. White⁸, M.J. White¹, D. Whiteson¹⁷⁰, B.W. Whitmore⁹⁰, W. Wiedenmann¹⁸⁰, C. Wiel⁴⁸, M. Wiersma¹⁴³, N. Wieseotte¹⁰⁰, C. Wigglesworth⁴⁰, L.A.M. Wiik-Fuchs⁵², H.G. Wilkens³⁶, L.J. Wilkins⁹⁴, H.H. Williams¹³⁶, S. Williams³², C. Willis¹⁰⁷, S. Willocq¹⁰³, I. Wingerter-Seez⁵, E. Winkels¹⁵⁵, F. Winklmeier¹³¹, B.T. Winter⁵², M. Wittgen¹⁵², M. Wobisch⁹⁶, A. Wolf¹⁰⁰, T.M.H. Wolf¹²⁰, R. Wolff¹⁰², R. Wölker¹³⁴, J. Wollrath⁵², M.W. Wolter⁸⁵, H. Wolters^{139a,139c}, V.W.S. Wong¹⁷⁴, N.L. Woods¹⁴⁵, S.D. Worm⁴⁶, B.K. Wosiek⁸⁵, K.W. Woźniak⁸⁵,

K. Wraight⁵⁷, S.L. Wu¹⁸⁰, X. Wu⁵⁴, Y. Wu^{60a}, T.R. Wyatt¹⁰¹, B.M. Wynne⁵⁰, S. Xella⁴⁰, Z. Xi¹⁰⁶, L. Xia¹⁷⁷, X. Xiao¹⁰⁶, I. Xiotidis¹⁵⁵, D. Xu^{15a}, H. Xu^{60a}, H. Xu^{60a}, L. Xu²⁹, T. Xu¹⁴⁴, W. Xu¹⁰⁶, Z. Xu^{60b}, Z. Xu¹⁵², B. Yabsley¹⁵⁶, S. Yacoub^{33a}, K. Yajima¹³², D.P. Yallup⁹⁵, N. Yamaguchi⁸⁸, Y. Yamaguchi¹⁶⁴, A. Yamamoto⁸², M. Yamatani¹⁶², T. Yamazaki¹⁶², Y. Yamazaki⁸³, J. Yan^{60c}, Z. Yan²⁵, H.J. Yang^{60c,60d}, H.T. Yang¹⁸, S. Yang^{60a}, T. Yang^{63c}, X. Yang^{60b,58}, Y. Yang¹⁶², Z. Yang^{60a}, W.-M. Yao¹⁸, Y.C. Yap⁴⁶, Y. Yasu⁸², E. Yatsenko^{60c,60d}, H. Ye^{15c}, J. Ye⁴², S. Ye²⁹, I. Yeletsikh⁸⁰, M.R. Yexley⁹⁰, E. Yigitbasi²⁵, K. Yorita¹⁷⁸, K. Yoshihara⁷⁹, C.J.S. Young³⁶, C. Young¹⁵², J. Yu⁷⁹, R. Yuan^{60b,h}, X. Yue^{61a}, M. Zaazoua^{35e}, B. Zabinski⁸⁵, G. Zacharis¹⁰, E. Zaffaroni⁵⁴, J. Zahreddine¹³⁵, A.M. Zaitsev^{123,ah}, T. Zakareishvili^{158b}, N. Zakharchuk³⁴, S. Zambito⁵⁹, D. Zanzi³⁶, D.R. Zaripovas⁵⁷, S.V. Zeißner⁴⁷, C. Zeitnitz¹⁸¹, G. Zemaityte¹³⁴, J.C. Zeng¹⁷², O. Zenin¹²³, T. Ženiš^{28a}, D. Zerwas⁶⁵, M. Zgubič¹³⁴, B. Zhang^{15c}, D.F. Zhang^{15b}, G. Zhang^{15b}, H. Zhang^{15c}, J. Zhang⁶, Kaili Zhang^{15a}, L. Zhang^{15c}, L. Zhang^{60a}, M. Zhang¹⁷², R. Zhang¹⁸⁰, S. Zhang¹⁰⁶, X. Zhang^{60c}, X. Zhang^{60b}, Y. Zhang^{15a,15d}, Z. Zhang^{63a}, Z. Zhang⁶⁵, P. Zhao⁴⁹, Z. Zhao^{60a}, A. Zhemchugov⁸⁰, Z. Zheng¹⁰⁶, D. Zhong¹⁷², B. Zhou¹⁰⁶, C. Zhou¹⁸⁰, H. Zhou⁷, M.S. Zhou^{15a,15d}, M. Zhou¹⁵⁴, N. Zhou^{60c}, Y. Zhou⁷, C.G. Zhu^{60b}, C. Zhu^{15a,15d}, H.L. Zhu^{60a}, H. Zhu^{15a}, J. Zhu¹⁰⁶, Y. Zhu^{60a}, X. Zhuang^{15a}, K. Zhukov¹¹¹, V. Zhulanov^{122b,122a}, D. Zieminska⁶⁶, N.I. Zimine⁸⁰, S. Zimmermann⁵², Z. Zinonos¹¹⁵, M. Ziolkowski¹⁵⁰, L. Živković¹⁶, G. Zobernig¹⁸⁰, A. Zoccoli^{23b,23a}, K. Zoch⁵³, T.G. Zorbas¹⁴⁸, R. Zou³⁷, L. Zwalinski³⁶

¹ Department of Physics, University of Adelaide, Adelaide; Australia

² Physics Department, SUNY Albany, Albany NY; United States of America

³ Department of Physics, University of Alberta, Edmonton AB; Canada

⁴ (a) Department of Physics, Ankara University, Ankara; (b) Istanbul Aydin University, Application and Research Center for Advanced Studies, Istanbul; (c) Division of Physics, TOBB University of Economics and Technology, Ankara; Turkey

⁵ LAPP, Université Grenoble Alpes, Université Savoie Mont Blanc, CNRS/IN2P3, Annecy; France

⁶ High Energy Physics Division, Argonne National Laboratory, Argonne IL; United States of America

⁷ Department of Physics, University of Arizona, Tucson AZ; United States of America

⁸ Department of Physics, University of Texas at Arlington, Arlington TX; United States of America

⁹ Physics Department, National and Kapodistrian University of Athens, Athens; Greece

¹⁰ Physics Department, National Technical University of Athens, Zografou; Greece

¹¹ Department of Physics, University of Texas at Austin, Austin TX; United States of America

¹² (a) Bahcesehir University, Faculty of Engineering and Natural Sciences, Istanbul; (b) Istanbul Bilgi University, Faculty of Engineering and Natural Sciences, Istanbul; (c) Department of Physics, Bogazici University, Istanbul; (d) Department of Physics Engineering, Gaziantep University, Gaziantep; Turkey

¹³ Institute of Physics, Azerbaijan Academy of Sciences, Baku; Azerbaijan

¹⁴ Institut de Física d'Altes Energies (IFAE), Barcelona Institute of Science and Technology, Barcelona; Spain

¹⁵ (a) Institute of High Energy Physics, Chinese Academy of Sciences, Beijing; (b) Physics Department, Tsinghua University, Beijing; (c) Department of Physics, Nanjing University, Nanjing;

(d) University of Chinese Academy of Science (UCAS), Beijing; China

¹⁶ Institute of Physics, University of Belgrade, Belgrade; Serbia

¹⁷ Department for Physics and Technology, University of Bergen, Bergen; Norway

¹⁸ Physics Division, Lawrence Berkeley National Laboratory and University of California, Berkeley CA; United States of America

¹⁹ Institut für Physik, Humboldt Universität zu Berlin, Berlin; Germany

²⁰ Albert Einstein Center for Fundamental Physics and Laboratory for High Energy Physics, University of Bern, Bern; Switzerland

²¹ School of Physics and Astronomy, University of Birmingham, Birmingham; United Kingdom

²² (a) Facultad de Ciencias y Centro de Investigaciones, Universidad Antonio Nariño, Bogotá; (b) Departamento de Física, Universidad Nacional de Colombia, Bogotá; Colombia

²³ (a) INFN Bologna and Università di Bologna, Dipartimento di Fisica; (b) INFN Sezione di Bologna; Italy

²⁴ Physikalisches Institut, Universität Bonn, Bonn; Germany

²⁵ Department of Physics, Boston University, Boston MA; United States of America

²⁶ Department of Physics, Brandeis University, Waltham MA; United States of America

²⁷ (a) Transilvania University of Brasov, Brasov; (b) Horia Hulubei National Institute of Physics and Nuclear Engineering, Bucharest; (c) Department of Physics, Alexandru Ioan Cuza University of Iasi, Iasi; (d) National Institute for Research and Development of Isotopic and Molecular Technologies, Physics Department, Cluj-Napoca; (e) University Politehnica Bucharest, Bucharest; (f) West University in Timisoara, Timisoara; Romania

²⁸ (a) Faculty of Mathematics, Physics and Informatics, Comenius University, Bratislava; (b) Department of Subnuclear Physics, Institute of Experimental Physics of the Slovak Academy of Sciences, Kosice; Slovak Republic

²⁹ Physics Department, Brookhaven National Laboratory, Upton NY; United States of America

³⁰ Departamento de Física, Universidad de Buenos Aires, Buenos Aires; Argentina

³¹ California State University, CA; United States of America

³² Cavendish Laboratory, University of Cambridge, Cambridge; United Kingdom

³³ (a) Department of Physics, University of Cape Town, Cape Town; (b) iThemba Labs, Western Cape; (c) Department of Mechanical Engineering Science, University of Johannesburg, Johannesburg; (d) University of South Africa, Department of Physics, Pretoria; (e) School of Physics, University of the Witwatersrand, Johannesburg; South Africa

³⁴ Department of Physics, Carleton University, Ottawa ON; Canada

³⁵ (a) Faculté des Sciences Ain Chock, Réseau Universitaire de Physique des Hautes Energies – Université Hassan II, Casablanca; (b) Faculté des Sciences, Université Ibn-Tofail, Kénitra;

(c) Faculté des Sciences Semlalia, Université Cadi Ayyad, LPHEA, Marrakech; (d) Faculté des Sciences, Université Mohamed Premier and LPTPM, Oujda; (e) Faculté des sciences, Université Mohammed V, Rabat; Morocco

³⁶ CERN, Geneva; Switzerland

³⁷ Enrico Fermi Institute, University of Chicago, Chicago IL; United States of America

³⁸ LPC, Université Clermont Auvergne, CNRS/IN2P3, Clermont-Ferrand; France

³⁹ Nevis Laboratory, Columbia University, Irvington NY; United States of America

⁴⁰ Niels Bohr Institute, University of Copenhagen, Copenhagen; Denmark

⁴¹ (a) Dipartimento di Fisica, Università della Calabria, Rende; (b) INFN Gruppo Collegato di Cosenza, Laboratori Nazionali di Frascati; Italy

⁴² Physics Department, Southern Methodist University, Dallas TX; United States of America

⁴³ Physics Department, University of Texas at Dallas, Richardson TX; United States of America

⁴⁴ National Centre for Scientific Research "Demokritos", Agia Paraskevi; Greece

⁴⁵ (a) Department of Physics, Stockholm University; (b) Oskar Klein Centre, Stockholm; Sweden

- ⁴⁶ Deutsches Elektronen-Synchrotron DESY, Hamburg and Zeuthen; Germany
- ⁴⁷ Lehrstuhl für Experimentelle Physik IV, Technische Universität Dortmund, Dortmund; Germany
- ⁴⁸ Institut für Kern- und Teilchenphysik, Technische Universität Dresden, Dresden; Germany
- ⁴⁹ Department of Physics, Duke University, Durham NC; United States of America
- ⁵⁰ SUPA – School of Physics and Astronomy, University of Edinburgh, Edinburgh; United Kingdom
- ⁵¹ INFN e Laboratori Nazionali di Frascati, Frascati; Italy
- ⁵² Physikalisches Institut, Albert-Ludwigs-Universität Freiburg, Freiburg; Germany
- ⁵³ II. Physikalisches Institut, Georg-August-Universität Göttingen, Göttingen; Germany
- ⁵⁴ Département de Physique Nucléaire et Corpusculaire, Université de Genève, Genève; Switzerland
- ⁵⁵ ^(a) Dipartimento di Fisica, Università di Genova, Genova; ^(b) INFN Sezione di Genova; Italy
- ⁵⁶ II. Physikalisches Institut, Justus-Liebig-Universität Giessen, Giessen; Germany
- ⁵⁷ SUPA – School of Physics and Astronomy, University of Glasgow, Glasgow; United Kingdom
- ⁵⁸ LPSC, Université Grenoble Alpes, CNRS/IN2P3, Grenoble INP, Grenoble; France
- ⁵⁹ Laboratory for Particle Physics and Cosmology, Harvard University, Cambridge MA; United States of America
- ⁶⁰ ^(a) Department of Modern Physics and State Key Laboratory of Particle Detection and Electronics, University of Science and Technology of China, Hefei; ^(b) Institute of Frontier and Interdisciplinary Science and Key Laboratory of Particle Physics and Particle Irradiation (MOE), Shandong University, Qingdao; ^(c) School of Physics and Astronomy, Shanghai Jiao Tong University, KLPPAC-MoE, SKLPPC, Shanghai; ^(d) Tsung-Dao Lee Institute, Shanghai; China
- ⁶¹ ^(a) Kirchhoff-Institut für Physik, Ruprecht-Karls-Universität Heidelberg, Heidelberg; ^(b) Physikalisches Institut, Ruprecht-Karls-Universität Heidelberg, Heidelberg; Germany
- ⁶² Faculty of Applied Information Science, Hiroshima Institute of Technology, Hiroshima; Japan
- ⁶³ ^(a) Department of Physics, Chinese University of Hong Kong, Shatin, N.T., Hong Kong; ^(b) Department of Physics, University of Hong Kong, Hong Kong; ^(c) Department of Physics and Institute for Advanced Study, Hong Kong University of Science and Technology, Clear Water Bay, Kowloon, Hong Kong; China
- ⁶⁴ Department of Physics, National Tsing Hua University, Hsinchu; Taiwan
- ⁶⁵ IJCLab, Université Paris-Saclay, CNRS/IN2P3, 91405, Orsay; France
- ⁶⁶ Department of Physics, Indiana University, Bloomington IN; United States of America
- ⁶⁷ ^(a) INFN Gruppo Collegato di Udine, Sezione di Trieste, Udine; ^(b) ICTP, Trieste; ^(c) Dipartimento Politecnico di Ingegneria e Architettura, Università di Udine, Udine; Italy
- ⁶⁸ ^(a) INFN Sezione di Lecce; ^(b) Dipartimento di Matematica e Fisica, Università del Salento, Lecce; Italy
- ⁶⁹ ^(a) INFN Sezione di Milano; ^(b) Dipartimento di Fisica, Università di Milano, Milano; Italy
- ⁷⁰ ^(a) INFN Sezione di Napoli; ^(b) Dipartimento di Fisica, Università di Napoli, Napoli; Italy
- ⁷¹ ^(a) INFN Sezione di Pavia; ^(b) Dipartimento di Fisica, Università di Pavia, Pavia; Italy
- ⁷² ^(a) INFN Sezione di Pisa; ^(b) Dipartimento di Fisica E. Fermi, Università di Pisa, Pisa; Italy
- ⁷³ ^(a) INFN Sezione di Roma; ^(b) Dipartimento di Fisica, Sapienza Università di Roma, Roma; Italy
- ⁷⁴ ^(a) INFN Sezione di Roma Tor Vergata; ^(b) Dipartimento di Fisica, Università di Roma Tor Vergata, Roma; Italy
- ⁷⁵ ^(a) INFN Sezione di Roma Tre; ^(b) Dipartimento di Matematica e Fisica, Università Roma Tre, Roma; Italy
- ⁷⁶ ^(a) INFN-TIFPA; ^(b) Università degli Studi di Trento, Trento; Italy
- ⁷⁷ Institut für Astro- und Teilchenphysik, Leopold-Franzens-Universität, Innsbruck; Austria
- ⁷⁸ University of Iowa, Iowa City IA; United States of America
- ⁷⁹ Department of Physics and Astronomy, Iowa State University, Ames IA; United States of America
- ⁸⁰ Joint Institute for Nuclear Research, Dubna; Russia
- ⁸¹ ^(a) Departamento de Engenharia Elétrica, Universidade Federal de Juiz de Fora (UFJF), Juiz de Fora; ^(b) Universidade Federal do Rio De Janeiro COPPE/EE/IF, Rio de Janeiro; ^(c) Universidade Federal de São João del Rei (UFSJ), São João del Rei; ^(d) Instituto de Física, Universidade de São Paulo, São Paulo; Brazil
- ⁸² KEK, High Energy Accelerator Research Organization, Tsukuba; Japan
- ⁸³ Graduate School of Science, Kobe University, Kobe; Japan
- ⁸⁴ ^(a) AGH University of Science and Technology, Faculty of Physics and Applied Computer Science, Krakow; ^(b) Marian Smoluchowski Institute of Physics, Jagiellonian University, Krakow; Poland
- ⁸⁵ Institute of Nuclear Physics Polish Academy of Sciences, Krakow; Poland
- ⁸⁶ Faculty of Science, Kyoto University, Kyoto; Japan
- ⁸⁷ Kyoto University of Education, Kyoto; Japan
- ⁸⁸ Research Center for Advanced Particle Physics and Department of Physics, Kyushu University, Fukuoka; Japan
- ⁸⁹ Instituto de Física La Plata, Universidad Nacional de La Plata and CONICET, La Plata; Argentina
- ⁹⁰ Physics Department, Lancaster University, Lancaster; United Kingdom
- ⁹¹ Oliver Lodge Laboratory, University of Liverpool, Liverpool; United Kingdom
- ⁹² Department of Experimental Particle Physics, Jožef Stefan Institute and Department of Physics, University of Ljubljana, Ljubljana; Slovenia
- ⁹³ School of Physics and Astronomy, Queen Mary University of London, London; United Kingdom
- ⁹⁴ Department of Physics, Royal Holloway University of London, Egham; United Kingdom
- ⁹⁵ Department of Physics and Astronomy, University College London, London; United Kingdom
- ⁹⁶ Louisiana Tech University, Ruston LA; United States of America
- ⁹⁷ Fysiska institutionen, Lunds universitet, Lund; Sweden
- ⁹⁸ Centre de Calcul de l'Institut National de Physique Nucléaire et de Physique des Particules (IN2P3), Villeurbanne; France
- ⁹⁹ Departamento de Física Teórica C-15 and CIAFF, Universidad Autónoma de Madrid, Madrid; Spain
- ¹⁰⁰ Institut für Physik, Universität Mainz, Mainz; Germany
- ¹⁰¹ School of Physics and Astronomy, University of Manchester, Manchester; United Kingdom
- ¹⁰² CPPM, Aix-Marseille Université, CNRS/IN2P3, Marseille; France
- ¹⁰³ Department of Physics, University of Massachusetts, Amherst MA; United States of America
- ¹⁰⁴ Department of Physics, McGill University, Montreal QC; Canada
- ¹⁰⁵ School of Physics, University of Melbourne, Victoria; Australia
- ¹⁰⁶ Department of Physics, University of Michigan, Ann Arbor MI; United States of America
- ¹⁰⁷ Department of Physics and Astronomy, Michigan State University, East Lansing MI; United States of America
- ¹⁰⁸ B.I. Stepanov Institute of Physics, National Academy of Sciences of Belarus, Minsk; Belarus
- ¹⁰⁹ Research Institute for Nuclear Problems of Byelorussian State University, Minsk; Belarus
- ¹¹⁰ Group of Particle Physics, University of Montreal, Montreal QC; Canada
- ¹¹¹ P.N. Lebedev Physical Institute of the Russian Academy of Sciences, Moscow; Russia
- ¹¹² National Research Nuclear University MEPhI, Moscow; Russia
- ¹¹³ D.V. Skobeltsyn Institute of Nuclear Physics, M.V. Lomonosov Moscow State University, Moscow; Russia
- ¹¹⁴ Fakultät für Physik, Ludwig-Maximilians-Universität München, München; Germany
- ¹¹⁵ Max-Planck-Institut für Physik (Werner-Heisenberg-Institut), München; Germany
- ¹¹⁶ Nagasaki Institute of Applied Science, Nagasaki; Japan
- ¹¹⁷ Graduate School of Science and Kobayashi-Maskawa Institute, Nagoya University, Nagoya; Japan
- ¹¹⁸ Department of Physics and Astronomy, University of New Mexico, Albuquerque NM; United States of America
- ¹¹⁹ Institute for Mathematics, Astrophysics and Particle Physics, Radboud University Nijmegen/Nikhef, Nijmegen; Netherlands
- ¹²⁰ Nikhef National Institute for Subatomic Physics and University of Amsterdam, Amsterdam; Netherlands

- ¹²¹ Department of Physics, Northern Illinois University, DeKalb IL; United States of America
- ¹²² ^(a) Budker Institute of Nuclear Physics and NSU, SB RAS, Novosibirsk; ^(b) Novosibirsk State University, Novosibirsk; Russia
- ¹²³ Institute for High Energy Physics of the National Research Centre Kurchatov Institute, Protvino; Russia
- ¹²⁴ Institute for Theoretical and Experimental Physics named by A.I. Alikhanov of National Research Centre “Kurchatov Institute”, Moscow; Russia
- ¹²⁵ Department of Physics, New York University, New York NY; United States of America
- ¹²⁶ Ochanomizu University, Otsuka, Bunkyo-ku, Tokyo; Japan
- ¹²⁷ Ohio State University, Columbus OH; United States of America
- ¹²⁸ Homer L. Dodge Department of Physics and Astronomy, University of Oklahoma, Norman OK; United States of America
- ¹²⁹ Department of Physics, Oklahoma State University, Stillwater OK; United States of America
- ¹³⁰ Palacký University, RPTM, Joint Laboratory of Optics, Olomouc; Czech Republic
- ¹³¹ Institute for Fundamental Science, University of Oregon, Eugene, OR; United States of America
- ¹³² Graduate School of Science, Osaka University, Osaka; Japan
- ¹³³ Department of Physics, University of Oslo, Oslo; Norway
- ¹³⁴ Department of Physics, Oxford University, Oxford; United Kingdom
- ¹³⁵ LPNHE, Sorbonne Université, Université de Paris, CNRS/IN2P3, Paris; France
- ¹³⁶ Department of Physics, University of Pennsylvania, Philadelphia PA; United States of America
- ¹³⁷ Konstantinov Nuclear Physics Institute of National Research Centre “Kurchatov Institute”, PNPI, St. Petersburg; Russia
- ¹³⁸ Department of Physics and Astronomy, University of Pittsburgh, Pittsburgh PA; United States of America
- ¹³⁹ ^(a) Laboratório de Instrumentação e Física Experimental de Partículas – LIP, Lisboa; ^(b) Departamento de Física, Faculdade de Ciências, Universidade de Lisboa, Lisboa; ^(c) Departamento de Física, Universidade de Coimbra, Coimbra; ^(d) Centro de Física Nuclear da Universidade de Lisboa, Lisboa; ^(e) Departamento de Física, Universidade do Minho, Braga; ^(f) Departamento de Física Teórica y del Cosmos, Universidad de Granada, Granada (Spain); ^(g) Dep Física and CEFITEC of Faculdade de Ciências e Tecnologia, Universidade Nova de Lisboa, Caparica; ^(h) Instituto Superior Técnico, Universidade de Lisboa, Lisboa; Portugal
- ¹⁴⁰ Institute of Physics of the Czech Academy of Sciences, Prague; Czech Republic
- ¹⁴¹ Czech Technical University in Prague, Prague; Czech Republic
- ¹⁴² Charles University, Faculty of Mathematics and Physics, Prague; Czech Republic
- ¹⁴³ Particle Physics Department, Rutherford Appleton Laboratory, Didcot; United Kingdom
- ¹⁴⁴ IRFU, CEA, Université Paris-Saclay, Gif-sur-Yvette; France
- ¹⁴⁵ Santa Cruz Institute for Particle Physics, University of California Santa Cruz, Santa Cruz CA; United States of America
- ¹⁴⁶ ^(a) Departamento de Física, Pontificia Universidad Católica de Chile, Santiago; ^(b) Universidad Andres Bello, Department of Physics, Santiago; ^(c) Instituto de Alta Investigación, Universidad de Tarapacá; ^(d) Departamento de Física, Universidad Técnica Federico Santa María, Valparaíso; Chile
- ¹⁴⁷ Department of Physics, University of Washington, Seattle WA; United States of America
- ¹⁴⁸ Department of Physics and Astronomy, University of Sheffield, Sheffield; United Kingdom
- ¹⁴⁹ Department of Physics, Shinshu University, Nagano; Japan
- ¹⁵⁰ Department Physik, Universität Siegen, Siegen; Germany
- ¹⁵¹ Department of Physics, Simon Fraser University, Burnaby BC; Canada
- ¹⁵² SLAC National Accelerator Laboratory, Stanford CA; United States of America
- ¹⁵³ Physics Department, Royal Institute of Technology, Stockholm; Sweden
- ¹⁵⁴ Departments of Physics and Astronomy, Stony Brook University, Stony Brook NY; United States of America
- ¹⁵⁵ Department of Physics and Astronomy, University of Sussex, Brighton; United Kingdom
- ¹⁵⁶ School of Physics, University of Sydney, Sydney; Australia
- ¹⁵⁷ Institute of Physics, Academia Sinica, Taipei; Taiwan
- ¹⁵⁸ ^(a) E. Andronikashvili Institute of Physics, Iv. Javakhishvili Tbilisi State University, Tbilisi; ^(b) High Energy Physics Institute, Tbilisi State University, Tbilisi; Georgia
- ¹⁵⁹ Department of Physics, Technion, Israel Institute of Technology, Haifa; Israel
- ¹⁶⁰ Raymond and Beverly Sackler School of Physics and Astronomy, Tel Aviv University, Tel Aviv; Israel
- ¹⁶¹ Department of Physics, Aristotle University of Thessaloniki, Thessaloniki; Greece
- ¹⁶² International Center for Elementary Particle Physics and Department of Physics, University of Tokyo, Tokyo; Japan
- ¹⁶³ Graduate School of Science and Technology, Tokyo Metropolitan University, Tokyo; Japan
- ¹⁶⁴ Department of Physics, Tokyo Institute of Technology, Tokyo; Japan
- ¹⁶⁵ Tomsk State University, Tomsk; Russia
- ¹⁶⁶ Department of Physics, University of Toronto, Toronto ON; Canada
- ¹⁶⁷ ^(a) TRIUMF, Vancouver BC; ^(b) Department of Physics and Astronomy, York University, Toronto ON; Canada
- ¹⁶⁸ Division of Physics and Tomonaga Center for the History of the Universe, Faculty of Pure and Applied Sciences, University of Tsukuba, Tsukuba; Japan
- ¹⁶⁹ Department of Physics and Astronomy, Tufts University, Medford MA; United States of America
- ¹⁷⁰ Department of Physics and Astronomy, University of California Irvine, Irvine CA; United States of America
- ¹⁷¹ Department of Physics and Astronomy, University of Uppsala, Uppsala; Sweden
- ¹⁷² Department of Physics, University of Illinois, Urbana IL; United States of America
- ¹⁷³ Instituto de Física Corpuscular (IFIC), Centro Mixto Universidad de Valencia – CSIC, Valencia; Spain
- ¹⁷⁴ Department of Physics, University of British Columbia, Vancouver BC; Canada
- ¹⁷⁵ Department of Physics and Astronomy, University of Victoria, Victoria BC; Canada
- ¹⁷⁶ Fakultät für Physik und Astronomie, Julius-Maximilians-Universität Würzburg, Würzburg; Germany
- ¹⁷⁷ Department of Physics, University of Warwick, Coventry; United Kingdom
- ¹⁷⁸ Waseda University, Tokyo; Japan
- ¹⁷⁹ Department of Particle Physics, Weizmann Institute of Science, Rehovot; Israel
- ¹⁸⁰ Department of Physics, University of Wisconsin, Madison WI; United States of America
- ¹⁸¹ Fakultät für Mathematik und Naturwissenschaften, Fachgruppe Physik, Bergische Universität Wuppertal, Wuppertal; Germany
- ¹⁸² Department of Physics, Yale University, New Haven CT; United States of America

^a Also at Borough of Manhattan Community College, City University of New York, New York NY; United States of America.

^b Also at CERN, Geneva; Switzerland.

^c Also at CPPM, Aix-Marseille Université, CNRS/IN2P3, Marseille; France.

^d Also at Département de Physique Nucléaire et Corpusculaire, Université de Genève, Genève; Switzerland.

^e Also at Departament de Física de la Universitat Autònoma de Barcelona, Barcelona; Spain.

^f Also at Department of Applied Physics and Astronomy, University of Sharjah, Sharjah; United Arab Emirates.

^g Also at Department of Financial and Management Engineering, University of the Aegean, Chios; Greece.

^h Also at Department of Physics and Astronomy, Michigan State University, East Lansing MI; United States of America.

ⁱ Also at Department of Physics and Astronomy, University of Louisville, Louisville, KY; United States of America.

^j Also at Department of Physics, Ben Gurion University of the Negev, Beer Sheva; Israel.

^k Also at Department of Physics, California State University, East Bay; United States of America.

- ^l Also at Department of Physics, California State University, Fresno; United States of America.
- ^m Also at Department of Physics, California State University, Sacramento; United States of America.
- ⁿ Also at Department of Physics, King's College London, London; United Kingdom.
- ^o Also at Department of Physics, St. Petersburg State Polytechnical University, St. Petersburg; Russia.
- ^p Also at Department of Physics, University of Adelaide, Adelaide; Australia.
- ^q Also at Department of Physics, University of Fribourg, Fribourg; Switzerland.
- ^r Also at Dipartimento di Matematica, Informatica e Fisica, Università di Udine, Udine; Italy.
- ^s Also at Faculty of Physics, M.V. Lomonosov Moscow State University, Moscow; Russia.
- ^t Also at Giresun University, Faculty of Engineering, Giresun; Turkey.
- ^u Also at Graduate School of Science, Osaka University, Osaka; Japan.
- ^v Also at Hellenic Open University, Patras; Greece.
- ^w Also at IJCLab, Université Paris-Saclay, CNRS/IN2P3, 91405, Orsay; France.
- ^x Also at Institutio Catalana de Recerca i Estudis Avancats, ICREA, Barcelona; Spain.
- ^y Also at Institut für Experimentalphysik, Universität Hamburg, Hamburg; Germany.
- ^z Also at Institute for Mathematics, Astrophysics and Particle Physics, Radboud University Nijmegen/Nikhef, Nijmegen; Netherlands.
- ^{aa} Also at Institute for Nuclear Research and Nuclear Energy (INRNE) of the Bulgarian Academy of Sciences, Sofia; Bulgaria.
- ^{ab} Also at Institute for Particle and Nuclear Physics, Wigner Research Centre for Physics, Budapest; Hungary.
- ^{ac} Also at Institute of Particle Physics (IPP), Vancouver; Canada.
- ^{ad} Also at Institute of Physics, Azerbaijan Academy of Sciences, Baku; Azerbaijan.
- ^{ae} Also at Instituto de Fisica Teorica, IFT-UAM/CSIC, Madrid; Spain.
- ^{af} Also at Joint Institute for Nuclear Research, Dubna; Russia.
- ^{ag} Also at Louisiana Tech University, Ruston LA; United States of America.
- ^{ah} Also at Moscow Institute of Physics and Technology State University, Dolgoprudny; Russia.
- ^{ai} Also at National Research Nuclear University MEPhI, Moscow; Russia.
- ^{aj} Also at Physics Department, An-Najah National University, Nablus; Palestine.
- ^{ak} Also at Physics Dept, University of South Africa, Pretoria; South Africa.
- ^{al} Also at Physikalisches Institut, Albert-Ludwigs-Universität Freiburg, Freiburg; Germany.
- ^{am} Also at The City College of New York, New York NY; United States of America.
- ^{an} Also at TRIUMF, Vancouver BC; Canada.
- ^{ao} Also at Università di Napoli Parthenope, Napoli; Italy.
- * Deceased.